

THE SURFACE BRIGHTNESS–COLOR RELATIONS BASED ON ECLIPSING BINARY STARS: TOWARD PRECISION BETTER THAN 1% IN ANGULAR DIAMETER PREDICTIONS.

DARIUSZ GRACZYK^{1,2,3}, PIOTR KONORSKI⁴, GRZEGORZ PIETRZYŃSKI^{3,2}, WOLFGANG GIEREN^{2,1}, JESPER STORM⁵,
NICOLAS NARDETTO⁶, ALEXANDRE GALLENNE⁷, PIERRE F. L. MAXTED⁸, PIERRE KERVELLA^{9,10}
AND ZBIGNIEW KOLACZKOWSKI¹¹

¹Millennium Institute of Astrophysics (MAS), Chile

²Universidad de Concepción, Departamento de Astronomía, Casilla 160-C, Concepción, Chile; darek@astro-udec.cl

³Centrum Astronomiczne im. Mikołaja Kopernika (CAMK), PAN, Bartycka 18, 00-716 Warsaw, Poland; darek@ncac.torun.pl

⁴Obserwatorium Astronomiczne, Uniwersytet Warszawski, Al. Ujazdowskie 4, 00-478, Warsaw, Poland

⁵Leibniz-Institut für Astrophysik Potsdam, An der Sternwarte 16, 14482 Potsdam, Germany

⁶Université Côte d'Azur, Observatoire de la Côte d'Azur, CNRS, Laboratoire Lagrange, UMR7293, Nice, France

⁷European Southern Observatory, Alonso de Córdova 3107, Casilla 19001, Santiago 19, Chile

⁸Astrophysics Group, Keele University, Staffordshire, ST5 5BG, UK

⁹Unidad Mixta Internacional Franco-Chilena de Astronomía (CNRS UMI 3386), Departamento de Astronomía, Universidad de Chile,

Camino El Observatorio 1515, Las Condes, Santiago, Chile

¹⁰LESIA (UMR 8109), Observatoire de Paris, PSL Research University, CNRS, UPMC, Univ. Paris-Diderot, 5 place Jules Janssen, 92195 Meudon, France and

¹¹Instytut Astronomiczny, Uniwersytet Wrocławski, Kopernika 11, 51-622 Wrocław, Poland

Draft version February 21, 2017

ABSTRACT

In this study we investigate the calibration of surface brightness–color (SBC) relations based solely on eclipsing binary stars. We selected a sample of 35 detached eclipsing binaries with trigonometric parallaxes from *Gaia* DR1 or *Hipparcos*, whose absolute dimensions are known with an accuracy better than 3% and that lie within 0.3 kpc from the Sun. For the purpose of this study, we used mostly homogeneous optical and near-infrared photometry based on the Tycho-2 and 2MASS catalogs. We derived geometric angular diameters for all stars in our sample with a precision better than 10%, and for 11 of them with a precision better than 2%. The precision of individual angular diameters of the eclipsing binary components is currently limited by the precision of the geometric distances ($\sim 5\%$ on average). However, by using a subsample of systems with the best agreement between their geometric and photometric distances, we derived the precise SBC relations based only on eclipsing binary stars. These relations have precisions that are comparable to the best available SBC relations based on interferometric angular diameters, and they are fully consistent with them. With very precise *Gaia* parallaxes becoming available in the near future, angular diameters with a precision better than 1% will be abundant. At that point, the main uncertainty in the total error budget of the SBC relations will come from transformations between different photometric systems, disentangling of component magnitudes, and for hot OB stars, the main uncertainty will come from the interstellar extinction determination. We argue that all these issues can be overcome with modern high-quality data and conclude that a precision better than 1% is entirely feasible.

Keywords: binaries: eclipsing

1. INTRODUCTION

The surface brightness–color (SBC) relations play a fundamental role in predicting angular diameters of stars and serve as an almost perfect tool for deriving precise distances to eclipsing binary stars. They have also been extremely useful in Baade–Wesselink techniques to determine the distances to classical Cepheid stars (e.g. Gieren et al. 1995; Fouqué & Gieren 1997; Storm et al. 2011). The SBC relations are commonly calibrated based on direct stellar angular diameters measured by means of ground-based interferometry (e.g. Kervella et al. 2004; di Benedetto 2005; Challouf et al. 2014; Boyajian et al. 2014). The precision of the SBC relations is gradually improving thanks to the ever-growing number of stars with interferometric angular diameters and to improvements in dealing with the limb darkening.

Eclipsing binaries with known trigonometric parallaxes can also be used to derive the SBC relation. This idea was first formulated and used by Lacy (1977): the combination of a geometric distance and stellar radius im-

mediately provides an angular diameter of a component of an eclipsing binary. This can later be used to derive a dependence of the radiative flux scale on color, expressed in terms of the surface brightness parameter or the effective temperature. Deriving angular diameters of eclipsing binary stars is significantly more complex than determining an angular diameter of a single star with interferometry. However, using eclipsing binaries usually has an important advantage: good control on the limb-darkening uncertainties, at least when the light curves are of sufficient quality (e.g. Popper 1984). Early attempts were constrained to the color $V - R$ (Lacy 1977; Barnes et al. 1978; Popper 1980) and were based on only on three eclipsing binary systems with secure trigonometric parallaxes.

When *Hipparcos* parallaxes became available, Popper (1998) analyzed 14 well-detached eclipsing binaries with the most accurate parallaxes and absolute dimensions to compare radiative flux scales defined by interferometry and eclipsing binary systems. However, this analysis was

made only for $(B-V)$ color and included eclipsing binaries with a significant amount of chromospheric activity. Nonetheless, Popper (1998) concluded that the SBC relation based on non-active eclipsing binaries seemed to be complementary to that based on interferometric angular diameters. Kruszewski & Semeniuk (1999) developed the idea of using a large number of eclipsing binaries with geometric distances from Hipparcos to precisely calibrate the SBC relations. They compiled an extensive list of promising eclipsing binaries in the solar neighborhood (up to 200 pc). Soon after, Semeniuk (2001) derived the SBC relation from a sample of 13 eclipsing binary stars with *Hipparcos* parallaxes and Strömgren photometry. The calibration was made for the $(b-y)$ color and compared with the relation by Popper (1998), which was mostly based on interferometric and lunar occultation angular diameter measurements. The samples agreed well, but the derived SBC relation had very large scatter.

The usefulness of eclipsing binaries for distance measurements was investigated by Jerzykiewicz (2001) by comparison of corrected trigonometric parallaxes and photometric distances, with the conclusion that EBs are excellent standard candles. Smalley et al. (2002) used 15 eclipsing binary stars with Hipparcos parallaxes to derive a fundamental temperature scale for A-type stars, and Bilir et al. (2008) presented a brief analysis of using eclipsing binary stars to calibrate the absolute magnitudes of stars as a function of some intrinsic colors. The most recent application of eclipsing binaries to derive the SBC relations known to us is the work by Bonneau et al. (2006), where the SBC relation was calibrated against $(V-K)$ color, but these authors used photometric distances to derive angular diameters (see our Sec. 3.6). Recently, Stassun & Torres (2016a,b) used more than 100 eclipsing binaries to investigate possible systematics in recent Gaia DR1 parallaxes (Gaia Collaboration 2016) and concluded that a likely systematic shift of -0.25 mas is presented in Gaia parallaxes. The shift is consistent with the systematic global error of 0.3 mas in the DR1 that was announced by the Gaia team.

The list of eclipsing binary systems reported by Kruszewski & Semeniuk (1999) is the basis for our programme of investigating eclipsing binaries and deriving the SBC relations. The first paper from our program was devoted to the IO Aqr system (Graczyk et al. 2015) and showed that unrecognized triples may bias the derivation of the SBC relations. Although the maximum-light contribution of the third component of IO Aqr is low and relatively well determined, the SBC calibrations would have substantial problems to reach a precision of about 1% for this system. In a following paper (Gallenne et al. 2016) we derived a very precise orbital parallax to TZ For that allowed us to perform a preliminary check of the precision of existing SBC relations. Our parallax measurement to TZ For is in perfect agreement with the photometric distance and the Gaia DR1 parallax. The work on TZ For is a part of our larger effort to determine very precise dynamical parallaxes to a number of long-period eclipsing binaries.

Here we present in detail the method of deriving the SBC relations based on eclipsing binary stars, and for the first time, we publish the precise relations that are based solely on eclipsing binaries. Sect. 2 characterizes a

sample of systems and describes the selection criteria and data we used. In Sect. 3 we present the method outline of our analysis. Sect. 4 contains results, and these are discussed in Sect. 5. The last section is devoted to final remarks.

2. THE SAMPLE

For the purpose of our work, we use a volume-limited ($d < 300$ pc) sample of detached eclipsing binaries with published high-quality light curve and radial velocity solutions. The sample is supposed to contain *standard* eclipsing binary systems for the purpose of accurate distance determination/validation and surface brightness calibration. We made an extensive search for suitable systems in the literature using the SIMBAD database (Wenger et al. 2000) and NASA ADS. Useful guidance in this measure is provided by the compilations done by Kruszewski & Semeniuk (1999), Bilir et al. (2008), Torres et al. (2010) and more recently by Eker et al. (2014), Southworth (2015) and Stassun & Torres (2016a). The final sample contains 34 systems and additionally AL Ari, a system for which our new analysis is as-yet unpublished (Konorski et al. 2017). Our intention is that the sample would serve as a reference catalogue for very precise determinations of the photometric distances, the angular diameters and the surface brightness. We put very strict conditions for including an eclipsing binary in our sample. As a part of a selection procedure we did an extensive consistency check of published physical parameters for every candidate system and in some cases recalculated fundamental parameters to make them more concordant with the observables. Table 1 presents the basic information about selected eclipsing binaries. The criteria are described in details below.

2.1. Proximity effects

No proximity effects larger than 0.03 mag. Although semi-detached or even contact configuration eclipsing binaries were suggested as good distance indicators (e.g. Wytke & Wilson 2002; Wilson et al. 2010), our experience shows that their physical parameters are usually much more model dependent and thus less robust than those coming from analysis of detached eclipsing binaries. In fact only well-detached systems offer very simple geometry where both stars can be treated as almost perfect spheres. This simplifies the analysis, as magnitudes and colors of the system are virtually constant outside eclipses.

2.2. Intrinsic variability

No intrinsic variability amplitude larger than 0.04 mag. Larger variability (spots, pulsations) over a given threshold may lead to some bias in the estimation of true photometric indices on a level of $>2\%$, so we removed all systems with an active or pulsating component from our sample (e.g. RS CVn stars, chromospheric activity). The only system retained is EF Aqr showing some spot activity on a secondary but only small changes in the combined out-of-eclipse light (Vos et al. 2012).

2.3. Absolute dimensions

Precision better than 3%. For the purpose of surface brightness calibration a knowledge of the physical radii is fundamental because combined with a distance it gives the angular diameters. We chose known systems with the most precise absolute dimensions. An average precision of the radii determination in the sample is $\sigma_R/R = 1.2\%$. This sample is useful for utilization of the present Gaia parallaxes. For the future Gaia releases expected to have precision better than 1% for all stars in our sample (de Bruijne et al. 2014) some of the systems will need to be reanalyzed in order to achieve precision better than 2% of radii determination or eventually will have to be removed from the sample i.e. V1229 Tau, FM Leo, FL Lyr, MY Cyg, VZ Cep, V821 Cas.

2.4. Geometric distance

Precision better than 10% within 300 pc horizon. We used trigonometric parallaxes from the recent Gaia Data Release 1 (Gaia Collaboration 2016), augmented with Hipparcos parallaxes (van Leeuwen 2007) for some bright and nearby systems. Even so, there are just a few eclipsing binaries in our sample with high precision trigonometric parallaxes (fractional uncertainty $\sigma_\pi/\pi < 2\%$). In the case of one system, TZ For, we utilized the orbital parallax determined by Gallenne et al. (2016) which is by a factor of 5 more precise than the Gaia DR1 parallax.

2.5. Temperature

Effective temperatures known to within 5%. We use them to build precise models of the systems and to calculate infrared light ratios. In this work we utilized also temperatures to derive photometric distances (by the flux scaling) as proxies of the true geometric distances. In general temperatures are important for determining auxiliary parameters (e.g. limb darkening) during light curve analysis and thus we preferred systems with well determined radiative properties.

2.6. Multiplicity

We excluded systems with confirmed third light in photometry/spectroscopy or known close bright companions affecting photometric indexes. CD Tau has a close K-type companion at a distance of $\sim 10''$. The light of the companion is present in the optical light curves analyzed by Ribas et al. (1999) but it was carefully accounted for in their analysis. The companion is far enough away to not influence the Tycho or 2MASS magnitudes. Also AI Phe has a fainter visual companion ($11''$), the presence of which was accounted for by Kirkby-Kent et al. (2016) in their analysis. The case of AI Phe is actually more complicated as this system has another, even closer, invisible companion inducing acceleration on a main binary system (M. Konacki - priv. com.). At this moment the nature of this companion is uncertain but spectroscopic data suggests an M type dwarf. In that case its luminosity can be completely neglected (even in NIR) and we included this system in our sample. RR Lyn is a proposed triple system with a companion of $0.1 M_\odot$ (Khaliullin & Khaliullina 2002). Even if the companion will be confirmed with future spectroscopic monitoring at the moment no third light is visible in high quality light curves (e.g. Khaliullin et al. 2001) and we retained this system in our sample.

2.7. Photometry

We decided to use homogenous non-saturated optical/infrared photometry from Tycho-2 and the Two Micron All Sky Survey.

2.7.1. Optical

We downloaded the optical *BV* Tycho-2 photometry (Høg et al. 2000) of the eclipsing binaries from VizieR (Ochsenbein et al. 2000)¹. β Aur, which is by far the brightest star in our sample, is the only star that lacks Tycho photometry. In this case we used Johnson photometry from a compilation by Mermilliod (1991). Tycho photometry was subsequently transformed into the Johnson system using the method outlined by Bessell (2000). For 6 systems Tycho-2 photometry leads to unexplainable shifts in the temperatures and surface brightness parameter derived so and we replaced it by more precise out-of-eclipse optical photometry from the literature.

2.7.2. Near infrared

We downloaded NIR *JHK_S* photometry of the Two Micron All Sky Survey (2MASS) (Skrutskie et al. 2006) from VizieR². Magnitudes were converted onto the Johnson system using equations given in Bessell & Brett (1988) and Carpenter (2001)³. The transformation equations are as follow:

$$\begin{aligned} K_J - K_{2M} &= 0.037 - 0.017(J - K)_{2M} - 0.007(V - K)_{2M} \\ (J - K)_J &= 1.064(J - K)_{2M} + 0.006 \\ (H - K)_J &= 1.096(H - K)_{2M} - 0.027 \end{aligned}$$

2MASS photometry of β Aur is saturated and we used Johnson *JK* photometry from a compilation by Ducati (2002). A lack of good NIR photometry forced us to remove from the sample the otherwise well suited system ψ Cen.

3. METHOD

3.1. The Wilson-Devinney model of the systems

For the purpose of obtaining homogenous parameters for the eclipsing binary sample we decided to create a model of each system. The models were built using the Wilson-Devinney code version 2007 (Wilson & Devinney 1971; Wilson 1979, 1990; van Hamme & Wilson 2007) while parameters of the models were based on solutions published in the literature. None of the eclipsing binaries in our sample has infrared *J, H, K* light curves suitable for deriving direct light ratios in those bands. Thus, in order to calculate intrinsic infrared colors of the components of each system we employed eclipsing binary models based on optical light curves and we extrapolated them into infrared. Such an approach may introduce some bias which will be discussed later in this paper. All models were checked for internal consistency of the parameters and it turned out that in many cases they had to be fine-tuned. In particular, the temperature ratio and the absolute temperature scale, being crucial for

¹ <http://vizier.u-strasbg.fr: I/259/tyc2>

² <http://vizier.u-strasbg.fr: II/281/2mass6x>

³ <http://www.astro.caltech.edu/~jmc/2mass/v3/transformations/>

Table 1
Basic data on the selected detached eclipsing binaries

Name	Tycho-2 ID	RA ₂₀₀₀ h:m:s	DEC ₂₀₀₀ deg:m:s	V ^a mag	Spectral Type	Ref. SpT	Orbital Period (d)	Ref. OrP	Parallax mas
YZ Cas	4307-2167-1	00:45:39.077	+74:59:17.06	5.653±0.015	A2m+F2V	1	4.4672235	36	10.30±0.49
AI Phe	8032-0625-1	01:09:34.195	-46:15:56.09	8.610±0.019	F8V+K0IV	8	24.592483	40	5.94±0.24
V505 Per	3690-0536-1	02:21:12.964	+54:30:36.28	6.889±0.016	F5V+F5V	2	4.222020	2	15.56±0.32
AL Ari	0645-1107-1	02:42:36.341	+12:44:07.77	9.223±0.034	F5V+G4V	3	3.7474543	3	7.11±0.37
V570 Per	3314-1225-1	03:09:34.944	+48:37:28.69	8.091±0.018	F3V+F5V	4	1.9009382	4	7.85±0.26
TZ For	7026-0633-1	03:14:40.093	-35:33:27.60	6.888±0.016	F7IV+G8III	5	75.66647	37	5.379±0.055 ^c
V1229 Tau ^d	1800-1622-1	03:47:29.454	+24:17:18.04	6.807±0.017	A0V+Am	6	2.46113408	38	7.57±0.40
V1094 Tau	1263-0642-1	04:12:03.593	+21:56:50.55	8.981±0.031	G0V+G2V	16	8.9885474	45	8.26±0.25
CD Tau	1291-0292-1	05:17:31.153	+20:07:54.63	6.768±0.016	F6V+F6V	7	3.435137	39	13.56±0.38
EW Ori	0104-1206-1	05:20:09.147	+02:02:39.97	9.902±0.043 ^e	F8V+G0V	16,47	6.9368432	47	5.48±0.23
UX Men	9378-0190-1	05:30:03.184	-76:14:55.35	8.251±0.017	F8V+F8V	9, 5	4.181100	41	9.72±0.21
TZ Men	9496-0590-1	05:30:13.886	-84:47:06.37	6.186±0.016	A0V+A8V	10, 5	8.56900	10	8.02±0.49
β Aur	2924-2742-1	05:59:31.723	+44:56:50.76	1.900±0.020 ^f	A1mIV+A1mIV	11,57	3.960047	42	40.21±0.23 ^b
RR Lyn	3772-2770-1	06:26:25.836	+56:17:06.35	5.558±0.015	A6mIV+F0V	12	9.945074	12	13.34±0.60 ^b
WW Aur	2426-0345-1	06:32:27.185	+32:27:17.63	5.832±0.016	A4m+A5m	13	2.5250194	43	11.03±0.50
HD 71636	2489-1972-1	08:29:56.311	+37:04:15.48	7.903±0.018	F2V+F5V	14	5.013292	14	8.40±0.40
VZ Hya	4874-0811-1	08:31:41.413	-06:19:07.56	8.953±0.027 ^g	F3V+F5V	21	2.9043002	51	6.94±0.24
KX Cnc	2484-0592-1	08:42:46.211	+31:51:45.37	7.192±0.017	F9V+F9V	15	31.2197874	44	20.54±0.38
PT Vel	7690-2859-1	09:10:57.720	-43:16:02.93	7.027±0.016	A0V+F0	17	1.802008	17	6.15±0.45
KW Hya	4891-1371-1	09:12:26.044	-07:06:35.38	6.100±0.016	A5m+F0V	18	7.750469	46	11.53±0.42 ^b
RZ Cha	9422-0104-1	10:42:24.104	-82:02:14.19	8.091±0.018	F5V+F5V	20	2.832084	48	5.68±0.26
FM Leo	0263-0727-1	11:12:45.095	+00:20:52.83	8.460±0.021	F7V+F7V	21	6.728606	49	7.00±0.32
GG Lup	7826-3079-1	15:18:56.376	-40:47:17.60	5.603±0.015	B7V+B9V	23	1.8495927	50	5.96±0.30 ^b
V335 Ser	0353-0301-1	15:59:05.756	+00:35:44.55	7.490±0.017	A1V+A3V	19	3.4498837	19	4.74±0.30
WZ Oph	0977-0216-1	17:06:39.042	+07:46:57.78	9.126±0.024	F8V+F8V	24, 25	4.183507	51	6.61±0.24
FL Lyr	3542-1492-1	19:12:04.862	+46:19:26.86	9.366±0.026	F8V+G8V	27	2.1781542	27	7.25±0.22
UZ Dra	4444-1595-1	19:25:55.045	+68:56:07.15	9.601±0.028	F7V+G0V	22	3.261302	52	5.21±0.25
V4089 Sgr	7936-2270-1	19:34:08.486	-40:02:04.70	5.907±0.016	A2IV+A7V	28, 29	4.6270956	29	6.75±0.49
V1143 Cyg	3938-1983-1	19:38:41.184	+54:58:25.65	5.889±0.015	F5V+F5V	30, 31	7.640742	54	24.75±0.35
MY Cyg	2680-1529-1	20:20:03.390	+33:56:35.02	8.341±0.019	F0m+F0m	32	4.0051870	55	3.95±0.24
EI Cep	4599-0082-1	21:28:28.206	+76:24:12.59	7.600±0.017	F3V+F1V	33	8.4393522	33	5.07±0.24
VZ Cep	4470-1334-1	21:50:11.135	+71:26:38.30	9.717±0.009 ^h	F3V+G4V	26	1.1833638	26	3.88±0.35
LL Aqr	5236-0883-1	22:34:42.152	-03:35:58.17	9.243±0.037 ⁱ	F8V+G2V	34	20.178321	56	7.75±0.27
EF Aqr	5248-1030-1	23:01:19.088	-06:26:15.35	9.885±0.022 ^j	F8V+G8V	15	2.8535721	53	5.06±0.50
W821 Cas	4001-1445-1	23:58:49.175	+53:40:19.81	8.286±0.017	A1V+A4	35	1.7697397	35	3.61±0.30

Note. — **Ref.** to Spectral Type (SpT) and/or Orbital Period (OrP): 1 - Pavlovski et al. (2014); 2 - Tomasella et al. (2008a); 3 - Konorski et al. (2017); 4 - Tomasella et al. (2008b); 5 - Torres et al. (2010); 6 - Abt & Levato (1978); 7 - Popper (1971); 8 - Andersen et al. (1988); 9 - Houk & Cowley (1975); 10 - Andersen et al. (1987a); 11 - Nordström & Johansen (1994b); 12 - Khaliullin et al. (2001); 13 - Kiyokawa & Kitamura (1975); 14 - Henry et al. (2006); 15 - this work; 16 - Nesterov et al. (1995); 17 - Bakiş et al. (2008); 18 - Andersen (1991); 19 - Lacy et al. (2012); 20 - Popper (1966); 21 - Houk & Swift (1999); 22 - Lacy et al. (1989); 23 - Andersen et al. (1993); 24 - Popper (1965); 25 - Batten et al. (1978); 26 - Torres & Lacy (2009); 27 - Popper et al. (1986); 28 - Houk (1978); 29 - Veramendi & González (2015); 30 - Hill et al. (1975); 31 - Andersen et al. (1987b); 32 - Malkov (1993); 33 - Torres et al. (2000); 34 - Griffin (2013); 35 - Çakırlı et al. (2009); 36 - Lacy (1981); 37 - Gallenne et al. (2016); 38 - David et al. (2016); 39 - Ribas et al. (1999); 40 - Kirkby-Kent et al. (2016); 41 - Clausen & Grønbech (1976); 42 - Southworth et al. (2007); 43 - Southworth et al. (2005); 44 - Sowell et al. (2012); 45 - Maxted et al. (2015); 46 - Andersen & Vaz (1984); 47 - Clausen et al. (2010); 48 - Jørgensen & Gyldenkerne (1975); 49 - Ratajczak et al. (2010); 50 - Budding et al. (2015); 51 - Clausen et al. (2008a); 52 - Gülmen et al. (1986); 53 - Vos et al. (2012); 54 - Giménez & Margrave (1985); 55 - Tucker et al. (2009); 56 - Southworth (2013); 57 - Lyubimkov et al. (1996)

^a Tycho-2 V_T magnitudes from Høg et al. (2000) converted onto Johnson V magnitudes using transformation given by Bessell (2000)

^b Hipparcos parallax (van Leeuwen 2007)

^c Orbital parallax from Gallenne et al. (2016), Hipparcos value $\varpi = 5.75 \pm 0.51$ mas, Gaia value $\varpi = 5.44 \pm 0.25$ mas

^d HD 23642, in the Pleiades cluster

^e Clausen et al. (2010)

^f Mermilliod (1991)

^g Clausen et al. (2008a)

^h Lacy (2002)

ⁱ Graczyk et al. (2016)

^j Vos et al. (2012)

precise prediction of infrared light ratios, were inspected carefully.

The procedure was as follows. For each system we collected orbital and photometric parameters from the most recent publications. The input parameters were the radial velocity semi-amplitudes $K_{1,2}$, the orbital period P , three parameters describing the position of the orbit (the orbital inclination i , the eccentricity e and the longitude of periastron ω), the photometric relative radii $r_{1,2}$ and the effective temperatures $T_{1,2}$. Those parameters were transformed into the semi-major axis of the system a , the mass ratio q and into dimensionless Roche potentials $\Omega_{1,2}$ using equations given in Torres et al. (2010) and Wilson (1979), i.e. parameters directly fitted or used within the WD program. We usually fixed the temperature of the primary star T_1 and then, using published light ratios in different photometric bands, we adjusted the temperature of the companion T_2 . In some cases however we also re-derived T_1 as it is described later. The rotation parameter $F_{1,2}$ was kept to 1 (synchronous rotation), unless there was a direct spectroscopic determination of F significantly different from unity. The albedo A and the gravity brightening g were set in a standard way for a convective atmosphere cooler than 7200 K and radiative ones for a hotter surface temperature. This was done only for the sake of consistency because the two parameters have negligible effect on the light ratios. The input and derived parameters used to create the appropriate WD models are listed in Table 2.

3.2. Correction of 2MASS magnitudes taken during eclipses

KX Cnc, GG Lup and WW Oph have 2MASS observations taken during the secondary eclipses. To account for a light lost during minima we used our models to calculate the appropriate corrections. The corrections are $\Delta J = -0.333$ mag, $\Delta H = -0.331$ mag and $\Delta K = -0.331$ mag for KX Cnc, $\Delta J = -0.277$ mag, $\Delta H = -0.281$ mag and $\Delta K = -0.285$ mag for GG Lup, $\Delta J = -0.392$ mag, $\Delta H = -0.390$ mag and $\Delta K = -0.390$ mag for WZ Oph. For GG Lup we accounted also for the apsidal motion which shifts the position of the eclipses (Wolf & Zejda 2005).

3.3. Temperature and Reddening

In some individual cases, described in the Appendix the temperature T_1 or/and color excess $E(B-V)$ were adjusted in order to obtain agreement between intrinsic colors and temperatures. Reddenings to each object were taken from the literature, if available, and also derived independently using the extinction maps by Schlegel et al. (1998) following the prescription given in Suchomska et al. (2015). Dereddened magnitudes and colors were calculated using the mean Galactic interstellar extinction curve from Fitzpatrick & Masana (2007) assuming $R_V = 3.1$. To re-derive temperatures we used a number of calibrations given below:

- $b-y$: Holmberg et al. (2007), Ramírez & Meléndez (2005), Alonso et al. (1996), Napiwotzki et al. (1993).
- $B - V$: Casagrande et al. (2010), González Hernández & Bonifacio (2009), Ramírez & Meléndez (2005), Flower (1996).

- $V - J$: Casagrande et al. (2010), González Hernández & Bonifacio (2009).
- $V - K$: Worthey & Lee (2011), Casagrande et al. (2010), González Hernández & Bonifacio (2009), Masana et al. (2006), Ramírez & Meléndez (2005), Houdashelt et al. (2000), Alonso et al. (1996).

3.4. Radial velocity semi-amplitudes

Usually we assumed radial velocity semi-amplitudes from the literature. When two or more orbital solutions were published based on different radial velocity sets and having uncertainties of the same order of magnitude, we used the weighted mean to derive the final parameters, i.e. AI Phe, EW Ori, UX Men, β Aur, GG Lup, UZ Dra, and V1143 Cyg. However, in few cases we redetermined the spectroscopic orbits from source data in order to derive directly $K_{1,2}$ or to check the consistency of the orbital parameters and their errors. The spectroscopic orbits were derived with the Wilson-Devinney code taking into account the full model of a system and all proximity effects. A set of numerical constants used to change from SI units into astrophysical units were chosen after Torres et al. (2010). Individual cases are described in the Appendix.

3.5. Distances

3.5.1. Geometric distances

The source of parallaxes is almost exclusively the recent release of Gaia parallaxes DR1 (Gaia Collaboration 2016) and in a few cases of close and bright systems where those parallaxes are unavailable we use parallaxes from the latest reduction of the Hipparcos data (van Leeuwen 2007). Distances are calculated through simple inversion of trigonometric parallaxes. It is known that this procedure for larger parallax errors ($\gtrsim 4\%$) is not unequivocal and must include some prior on expected space distribution of an object (e.g. Sandage & Saha 2002; Bailer-Jones 2015). Existence of this prior is necessary to recover a true distribution (distances) from an observed distribution (parallaxes) in the presence of observational errors. In terms of absolute luminosity bias it leads to the so called Lutz-Kelker correction (Lutz & Kelker 1973). However errors given by the Gaia DR1 are preliminary and likely overestimated (e.g. Casertano et al. 2016) and using them for parallax corrections would introduce unknown amounts of systematics. For the purpose of this paper we decided to not apply Lutz-Kelker corrections to the distances, especially as any such correction would be smaller than quoted errors. The resulting distances are summarized in Tab. 3.

3.5.2. Photometric distances

We employed the so-called standard method utilizing V-band bolometric corrections to derive photometric distances, known also as the bolometric flux scaling. We calculated distance d to the i -th component of the system using equation:

$$d_i(\text{pc}) = 3.360 \cdot 10^{-8} R_i T_i^2 10^{0.2(BC_i + V_i)}, \quad (1)$$

where index $i = \{1, 2\}$, R is the radius of a component in solar radii, T is its effective temperature in K, BC is a bolometric correction interpolated from the Flower

Table 2
Parameters of the Wilson-Devinney models

Eclipsing binary	RV semiamplitude		Input parameters			Fractional radius		Effective temperature		Reference	Model parameters			
	K_1 (km s ⁻¹)	K_2 (km s ⁻¹)	Orientation of the orbit			r_1	r_2	T_1 (K)	T_2 (K)		Semimajor axis (R_\odot)	Mass ratio	Ω_1	Ω_2
			e	ω (rad)	i (deg)									
YZ Cas	73.05(19)	124.78(27)	0.0	0.0	88.33(7)	0.14456(56)	0.07622(33)	9520(120)	6880(240)	2	17.4764	0.5854	7.5141	8.8912
AI Phe ^d	51.128(28)	49.120(19)	0.187(3)	1.933(6)	88.55(5)	0.03845(35)	0.06070(27)	6175(150)	5140(120)	3,4,5,1	47.8850	1.0409	27.290	18.361
V505 Per	89.01(8)	90.28(9)	0.0	0.0	87.95(4)	0.0860(9)	0.0846(9)	6512(21)	6460(30)	6	14.9724	0.9859	12.618	12.665
AL Ari	76.98(13)	98.38(21)	0.051(3)	1.20(2)	89.48(6)	0.1060(4)	0.0696(3)	6300(80)	5412(80)	7	12.9738	0.7825	10.269	12.411
V570 Per ^a	114.09(27)	122.48(28)	0.0	0.0	77.4(3)	0.1675(31)	0.1526(19)	6842(30)	6562(30)	8,1	9.10738	0.9315	6.9200	7.1538
TZ For ^b	40.868(11)	38.900(22)	0.0	0.0	85.66(4)	0.03320(70)	0.06972(92)	6350(70)	4930(30)	9,10	119.650	1.0506	31.416	16.046
V1229 Tau	99.02(27)	140.86(36)	0.0	0.0	78.2(1)	0.1450(23)	0.1262(37)	9950(300)	7640(300)	11,12	11.9214	0.7030	7.6115	6.7280
V1094 Tau ^c	65.38(7)	70.83(12)	0.2677(4)	5.822(3)	88.21(1)	0.06050(24)	0.04744(29)	5850(100)	5720(100)	13,1	23.3292	0.9231	17.792	20.863
CD Tau	96.8(5)	102.1(5)	0.0	0.0	87.7(3)	0.1330(10)	0.1172(13)	6200(50)	6194(50)	14	13.5172	0.9481	8.4785	9.1246
EW Ori ^c	72.48(21)	75.45(25)	0.076(2)	5.40(2)	89.86(9)	0.05786(18)	0.05434(18)	6070(95)	5875(95)	15,16,17,1	20.2258	0.9607	18.325	18.783
UX Men ^c	87.36(17)	90.08(14)	0.003(3)	1.3(6)	89.6(1)	0.0918(9)	0.0868(9)	6200(100)	6127(100)	18,3,1	14.6652	0.9682	11.871	12.196
TZ Men	62.15(12)	102.82(45)	0.035(7)	4.75(2)	88.7(1)	0.0722(7)	0.0513(5)	10400(500)	7240(300)	19	27.9328	0.6045	14.480	13.018
β Aur ^c	108.04(10)	110.93(10)	0.0018(4)	1.579(5)	76.8(1)	0.15694(81)	0.14595(82)	9350(200)	9297(200)	20,21,22,23,1	17.6051	0.9739	7.3643	7.7040
RR Lyn	65.65(6)	83.92(17)	0.079(1)	3.14(1)	87.5(1)	0.0878(5)	0.0541(11)	7570(120)	6980(100)	24,25	29.340	0.7823	12.244	15.657
WW Aur ^d	116.81(23)	126.49(28)	0.0	0.0	87.55(4)	0.1586(9)	0.1515(9)	8180(260)	7872(250)	26,1	12.1546	0.9235	7.2450	7.1487
HD 71636 ^a	80.30(18)	94.45(19)	0.0	0.0	85.63(2)	0.0904(5)	0.0784(5)	6950(140)	6440(140)	27,1	17.3682	0.8502	11.917	11.923
VZ Hya	94.92(19)	105.31(34)	0.0	0.0	88.88(9)	0.1143(4)	0.0968(6)	6645(150)	6300(150)	28	11.4972	0.9013	9.6587	10.367
KX Cnc ^{a,d}	50.039(65)	50.503(65)	0.4667(1)	1.113(1)	89.83(1)	0.01940(4)	0.01913(5)	6050(110)	5995(110)	29,1	54.8787	0.9908	53.405	53.674
PT Vel	117.2(2)	158.5(5)	0.127(6)	5.06(1)	88.2(5)	0.215(2)	0.160(2)	9250(150)	7650(155)	30	9.7457	0.7394	5.5259	5.9125
KW Hya ^c	70.12(21)	93.17(79)	0.0945(1)	3.929(2)	87.65(4)	0.0853(5)	0.0594(8)	8000(200)	6960(210)	31,1	24.9247	0.7526	12.559	13.908
RZ Cha ^d	108.2(6)	107.6(9)	0.0	0.0	82.89(7)	0.1777(20)	0.1893(40)	6580(150)	6530(150)	32,33,1	12.1746	1.0056	6.6545	6.3340
FM Leo	76.62(27)	78.46(28)	0.0	0.0	87.98(6)	0.0798(21)	0.0732(24)	6316(240)	6190(210)	34	20.6392	0.9765	13.505	14.354
GG Lup ^c	125.1(5)	203.4(8)	0.154(5)	2.351(3)	86.8(1)	0.2003(18)	0.1456(14)	14750(450)	11200(500)	35,36,1	11.8871	0.6150	5.7696	5.6076
V335 Ser	106.57(12)	120.07(38)	0.141(2)	1.139(7)	87.2(2)	0.1325(17)	0.1131(22)	9020(150)	8500(150)	37	15.3191	0.8876	8.5918	9.0764
WZ Oph ^d	88.77(19)	89.26(24)	0.0	0.0	89.1(1)	0.0952(8)	0.0964(8)	6232(100)	6212(100)	28,1	14.7240	0.9945	11.505	11.326
FL Lyr ^c	93.5(5)	118.9(7)	0.0	0.0	86.3(4)	0.140(3)	0.105(3)	6150(120)	5270(110)	15,1	9.1640	0.7864	7.9411	8.6028
UZ Dra ^d	93.52(35)	101.55(43)	0.0	0.0	89.1(2)	0.103(2)	0.091(2)	6450(120)	6170(120)	38,39,1	12.5768	0.9209	10.637	11.165
V4089 Sgr ^a	78.48(18)	126.20(24)	0.0	0.0	83.48(6)	0.2104(9)	0.0852(3)	8433(100)	7361(105)	40,1	18.8426	0.6219	5.3991	8.4925
V1143 Cyg	88.02(5)	89.97(10)	0.5378(3)	0.860(1)	87.0(1)	0.059(1)	0.058(1)	6450(100)	6400(100)	41,42	22.6950	0.9783	19.069	19.045
MY Cyg	101.9(8)	103.3(6)	0.010(1)	1.21(4)	88.58(2)	0.138(3)	0.134(3)	7050(200)	7000(200)	43,44,45	16.2482	0.9867	8.2580	8.3912
EI Cep ^c	76.84(13)	81.02(13)	0.0	0.0	87.23(9)	0.1099(20)	0.0884(18)	6750(120)	6977(120)	46,1	26.3649	0.9484	10.056	11.760
VZ Cep ^c	118.88(22)	150.48(67)	0.0	0.0	79.97(5)	0.2398(17)	0.1630(61)	6690(160)	5705(120)	47,1	6.3985	0.7900	4.9955	5.9680
LL Aqr	49.948(13)	57.736(14)	0.3165(1)	2.714(1)	89.55(3)	0.03246(5)	0.02459(8)	6080(50)	5705(60)	48,49	40.7438	0.8651	32.074	36.708
EF Aqr ^a	84.175(66)	110.66(24)	0.0	0.0	88.45(8)	0.1222(9)	0.0876(7)	6150(65)	5185(110)	50,1	10.9940	0.7607	8.9529	9.8076
V821 Cas ^a	120.8(1.7)	152.4(2.0)	0.127(7)	2.71(7)	82.6(1)	0.2434(13)	0.1466(17)	9400(400)	8600(400)	51,1	9.5600	0.7927	5.0538	6.6690

Note. — Reference: 1 - this paper; 2 - Pavlovski et al. (2014); 3 - Helminiak et al. (2009); 4 - Andersen et al. (1988); 5 - Kirkby-Kent et al. (2016); 6 - Tomasella et al. (2008a); 7 - Konorski et al. (2017); 8 - Tomasella et al. (2008b); 9 - Andersen et al. (1991); 10 - Gallenne et al. (2016); 11 - David et al. (2016); 12 - Groenewegen et al. (2007); 13 - Maxted et al. (2015); 14 - Ribas et al. (1999); 15 - Popper et al. (1986); 16 - Imbert (2002); 17 - Clausen et al. (2010); 18 - Andersen et al. (1989); 19 - Andersen et al. (1987a); 20 - Smith (1948); 21 - Behr et al. (2011); 22 - Nordström & Johansen (1994b); 23 - Southworth et al. (2007); 24 - Tomkin & Fekel (2006); 25 - Khaliullin et al. (2001); 26 - Southworth et al. (2005); 27 - Henry et al. (2006); 28 - Clausen et al. (2008b); 29 - Sowell et al. (2012); 30 - Bakiş et al. (2008); 31 - Andersen & Vaz (1984); 32 - Andersen et al. (1975); 33 - Giuricin et al. (1980); 34 - Ratajczak et al. (2010); 35 - Andersen et al. (1993); 36 - Budding et al. (2015); 37 - Lacy et al. (2012); 38 - Imbert (1986); 39 - Lacy et al. (1989); 40 - Veramendi & González (2015); 41 - Albrecht et al. (2007); 42 - Andersen et al. (1987b); 43 - Popper (1971); 44 - Tucker et al. (2009); 45 - Torres et al. (2010); 46 - Torres et al. (2000); 47 - Torres & Lacy (2009); 48 - Southworth (2013); 49 - Graczyk et al. (2016); 50 - Vos et al. (2012); 51 - Çakırlı et al. (2009)

^a We recalculated radial velocity semiamplitudes - see Section 3.4.

^b We set rotation parameter $F_1 = 18.0$

^c We adjusted temperature T_2 .

^d We recalculated both temperatures - see Section 3.3

Table 3
Photometric and physical parameters used to derive individual angular diameters and colors.

Eclipsing binary	$E(B-V)$ mag	Ref.	Radius (R_{\odot})		Distance (pc)		σ	Unreddened Johnson photometry ^a (mag)					Light ratio L_2/L_1 ^b				
			R_1	R_2	Geom.	Photom. ^c		B_0	V_0	J_0	H_0	K_0	B	V	J	H	K
YZ Cas	0.015(10)	1	2.526(11)	1.332(6)	97.1(4.6)	99.2(4.0)	0.35	5.657(48)	5.607(34)	5.616(21)	5.652(42)	5.635(22)	0.0610	0.0882	0.1682	0.2004	0.2046
AI Phe	0.012(10)	2,1	1.841(17)	2.907(13)	168.4(6.8)	167.9(6.7)	0.15	9.212(52)	8.573(36)	7.345(25)	6.930(38)	6.832(27)	0.7382	1.0057	1.6394	1.9685	1.9828
V505 Per	0.003(5)	1	1.288(14)	1.267(14)	64.3(1.3)	60.7(9)	2.23	7.287(34)	6.880(22)	6.117(70)	5.791(40)	5.794(21)	0.9244	0.9348	0.9522	0.9584	0.9588
AL Ari	0.012(10)	3	1.375(6)	0.903(4)	140.6(7.3)	137.0(4.0)	0.45	9.696(69)	9.186(46)	8.235(23)	7.933(23)	7.905(27)	0.1646	0.2100	0.3087	0.3571	0.3597
V570 Per	0.070(30)	1	1.525(30)	1.390(19)	127.4(4.2)	118.6(5.4)	1.29	8.270(126)	7.875(94)	7.156(35)	6.921(23)	6.888(22)	0.6567	0.6950	0.7645	0.7916	0.7926
TZ For	0.015(5)	4	3.972(84)	8.34(11)	185.9(1.9)	185.2(3.8)	0.17	7.569(34)	6.842(22)	5.530(21)	5.124(26)	5.007(30)	0.7888	1.2341	2.4644	3.1856	3.2193
V1229 Tau	0.020(10)	5,6	1.729(27)	1.505(45)	132.1(7.0)	133.1(7.5)	0.10	6.784(50)	6.745(35)	6.663(25)	6.644(29)	6.637(25)	0.2628	0.3385	0.5223	0.5800	0.5917
V1094 Tau	0.026(10)	7	1.411(6)	1.107(7)	121.1(3.7)	118.0(3.8)	0.58	9.575(66)	8.901(44)	7.814(23)	7.520(46)	7.437(22)	0.5318	0.5524	0.5851	0.5980	0.5986
CD Tau	0.005(5)	8,1	1.798(17)	1.584(20)	73.7(2.1)	68.6(1.2)	2.22	7.231(34)	6.753(22)	5.894(22)	5.671(34)	5.612(30)	0.7702	0.7724	0.7749	0.7764	0.7760
EW Ori	0.026(14)	9	1.170(5)	1.099(5)	182.5(7.7)	173.8(6.3)	0.88	10.407(94)	9.822(61)	8.837(26)	8.598(69)	8.513(22)	0.7209	0.7595	0.8223	0.8474	0.8486
UX Men	0.027(10)	10	1.346(13)	1.273(13)	102.9(2.2)	100.6(2.9)	0.62	8.692(50)	8.168(35)	7.222(29)	6.966(30)	6.931(25)	0.8318	0.8476	0.8721	0.8818	0.8822
TZ Men	0.000(5)	11	2.017(20)	1.433(15)	124.7(7.6)	117.7(8.2)	0.63	6.166(34)	6.186(22)	6.180(31)	6.128(44)	6.153(27)	0.1150	0.1623	0.3002	0.3508	0.3607
beta Aur	0.000(3)	1	2.763(15)	2.569(15)	24.9(1)	25.0(9)	0.26	1.930(34)	1.900(22)	1.869(42)	—	1.859(41)	0.8462	0.8524	0.8585	0.8597	0.8603
RR Lyn	0.007(5)	1	2.576(20)	1.587(30)	75.0(3.4)	72.6(2.0)	0.50	5.764(33)	5.536(22)	—	5.073(23)	5.021(17)	0.2343	0.2645	0.3298	0.3534	0.3541
WW Aur	0.008(5)	1	1.928(11)	1.841(11)	90.7(4.1)	85.8(4.0)	1.02	5.976(34)	5.807(22)	5.533(22)	5.505(29)	5.513(22)	0.7600	0.7953	0.8607	0.8753	0.8789
HD71636	0.020(10)	12	1.570(9)	1.362(7)	119.0(5.7)	118.6(4.1)	0.07	8.223(51)	7.841(36)	7.104(22)	6.917(24)	6.907(35)	0.4910	0.5442	0.6474	0.6886	0.6911
VZ Hya	0.027(20)	13	1.314(5)	1.113(7)	144.1(5.0)	146.0(7.3)	0.23	9.307(93)	8.870(67)	8.105(29)	7.844(28)	7.801(18)	0.5254	0.5683	0.6439	0.6747	0.6766
KX Cnc	0.001(5)	1	1.065(2)	1.050(3)	48.7(9)	49.0(1.4)	0.19	7.766(35)	7.189(23)	6.223(32)	5.949(30)	5.905(31)	0.9196	0.9330	0.9537	0.9616	0.9621
PT Vel	0.005(5)	14	2.095(20)	1.559(20)	163(12)	164.8(4.9)	0.19	7.062(34)	7.012(22)	6.902(32)	6.861(32)	6.871(30)	0.2395	0.2949	0.4199	0.4580	0.4641
KW Hya	0.006(6)	1	2.126(15)	1.480(22)	86.7(3.2)	86.5(3.6)	0.05	6.308(37)	6.081(24)	5.694(24)	5.642(44)	5.574(22)	0.2249	0.2699	0.3816	0.4221	0.4255
RZ Cha	0.038(20)	1	2.163(20)	2.305(20)	176.1(8.1)	179.4(8.0)	0.37	8.384(87)	7.974(64)	7.148(35)	6.926(40)	6.919(39)	1.0879	1.0988	1.1177	1.1241	1.1250
FM Leo	0.019(10)	1	1.648(43)	1.511(49)	142.9(6.5)	139.6(8.8)	0.27	8.884(53)	8.401(37)	7.554(23)	7.324(56)	7.229(24)	0.7441	0.7681	0.8062	0.8216	0.8222
GG Lup	0.027(10)	15	2.381(22)	1.732(17)	167.8(8.4)	147.3(9.5)	1.61	5.386(48)	5.520(34)	5.861(32)	5.980(38)	5.961(31)	0.3026	0.3236	0.3774	0.3875	0.3964
V335 Ser	0.068(8)	16	2.030(26)	1.733(34)	211(13)	195.2(6.0)	1.15	7.352(43)	7.280(30)	7.127(23)	7.105(36)	7.080(22)	0.5730	0.6109	0.6720	0.6870	0.6901
WZ Oph	0.030(16)	1	1.402(12)	1.420(12)	151.3(5.5)	164.9(5.7)	1.72	9.543(76)	9.033(55)	8.208(34)	7.972(37)	7.894(31)	1.0068	1.0115	1.0188	1.0214	1.0217
FL Lyr	0.010(7)	1	1.283(30)	0.962(30)	137.9(4.2)	131.9(5.2)	0.83	9.875(52)	9.335(34)	8.285(28)	7.983(36)	7.917(21)	0.2065	0.2646	0.3969	0.4623	0.4661
UZ Dra	0.012(7)	17	1.295(25)	1.144(25)	191.9(9.2)	189.7(6.6)	0.20	10.036(54)	9.564(35)	8.653(22)	8.423(22)	8.393(20)	0.5991	0.6411	0.7124	0.7419	0.7431
V4089 Sgr	0.027(15)	1	3.964(20)	1.605(7)	148(11)	145.5(4.3)	0.19	5.889(67)	5.824(49)	5.710(25)	5.627(40)	5.623(25)	0.0776	0.0953	0.1327	0.1452	0.1466
V1143 Cyg	0.000(5)	18,1	1.339(23)	1.316(23)	40.4(6)	39.2(1.1)	1.02	6.347(34)	5.889(22)	5.024(21)	4.845(22)	4.798(21)	0.9233	0.9339	0.9512	0.9577	0.9581
MY Cyg	0.048(30)	19	2.242(50)	2.178(50)	253(15)	229(14)	1.17	8.520(126)	8.193(94)	7.702(51)	7.563(46)	7.538(26)	0.9075	0.9158	0.9312	0.9360	0.9363
EI Cep	0.007(5)	20	2.898(48)	2.331(44)	197.2(9.3)	194.0(5.8)	0.30	7.956(35)	7.578(23)	6.879(21)	6.738(37)	6.696(18)	0.7702	0.7405	0.6891	0.6742	0.6723
VZ Cep	0.044(10)	21	1.534(12)	1.043(39)	258(23)	211.1(8.5)	2.07	10.025(46)	9.581(32)	8.796(23)	8.621(33)	8.606(22)	0.1764	0.2256	0.3308	0.3830	0.3851
LL Aqr	0.018(14)	22	1.323(6)	1.002(5)	129.0(4.5)	132.4(3.6)	0.57	9.748(86)	9.187(57)	8.180(26)	7.864(37)	7.836(24)	0.3848	0.4268	0.4998	0.5306	0.5320
EF Aqr	0.025(15)	23	1.343(10)	0.963(8)	198(20)	169.4(6.0)	1.57	10.385(77)	9.808(51)	8.849(27)	8.511(29)	8.496(24)	0.1678	0.2207	0.3480	0.4141	0.4174
V821 Cas	0.060(30)	1	2.327(29)	1.401(33)	277(23)	306(24)	0.91	8.158(125)	8.101(94)	7.976(29)	7.994(32)	7.975(29)	0.2554	0.2829	0.3231	0.3333	0.3354

Note. — References to reddening: 1 - this work; 2 - Hrivnak & Milone (1984); 3 - Konorski et al. (2017); 4 - Gallenne et al. (2016); 5 - Munari et al. (2004); 6 - Groenewegen et al. (2007); 7 - Maxted et al. (2015); 8 - Ribas et al. (1999); 9 - Clausen et al. (2010); 10 - Andersen et al. (1989); 11 - Andersen et al. (1987a); 12 - Henry et al. (2006); 13 - Clausen et al. (2008b); 14 - Bakış et al. (2008); 15 - Andersen et al. (1993); 16 - Lacy et al. (2012); 17 - Ammons et al. (2006); 18 - Andersen et al. (1987b); 19 - Popper & Etzel (1981); 20 - Torres et al. (2000); 21 - Torres & Lacy (2009); 22 - Graczyk et al. (2016); 23 - Vos et al. (2012)

^a Combined, extinction-corrected, out-of-eclipse magnitudes of both components expressed in Johnson photometric system.

^b Calculated using the WD model.

^c Photometric distances derived from bolometric flux scaling.

(1996) tables for a given temperature and V is the intrinsic magnitude of a component (corrected for extinction). The distance to a particular system was calculated as the unweighted average distance of the two components. The purposes of introducing photometric distances is to check for consistency of the eclipsing binary model parameters and validation of the Gaia parallaxes used in the analysis. The photometric distances are given in Tab. 3.

3.6. Angular diameters

In order to derive surface brightness – color relations we need to calculate individual angular diameters of the stars. Angular diameters are calculated with the formula:

$$\phi(\text{mas}) = 9.3004 \cdot R(R_{\odot})/d(\text{pc}), \quad (2)$$

where d is a distance, R the radius of the star and the conversion factor is equal to $2000R_{\odot}/1\text{AU}$ assuming a solar radius $R_{\odot} = 695660$ km (Habbereiter et al. 2008) and a length of the astronomical unit $1\text{AU} = 149597871$ km (Pitjeva & Standish 2009).

We emphasize that angular diameter calculated from the photometric distance is a function of *radiative* properties of a star (mainly its effective temperature) and not its *geometric* properties. Indeed, if we combine equations 1 and 2 we derive angular diameter which is only a function of the effective temperature, the V -band bolometric correction (also temperature dependent) and extinction corrected V -band magnitude. Because of this we do not utilize the photometric distances to calculate angular diameters in the present work.

3.7. Intrinsic magnitudes

In Table 3 we summarize all parameters used to derive the intrinsic photometric indexes of components. The mean galactic extinction curve with $R_V = 3.1$ (Fitzpatrick & Masana 2007) was used to correct the observed magnitudes for reddening. Next, with the help of our WD models, we calculated light ratios in the Johnson $BVJHK$ bands and use them to derive intrinsic magnitudes and colors of each component. The WD code uses an atmospheric approximation with intensities based on ATLAS9 (Kurucz 1993) model stellar atmospheres which are integrated over a given passband to give emerging flux being expressed as fraction of flux emerging from the black body of the same temperature. For all the systems in our sample B and V light ratios are tuned to published light ratios based on literature light curve solutions. However in order to calculate the light ratios in the infrared JHK bands we need to extrapolate the models as none of the systems has infrared light curves published or analyzed. This is why the temperature ratio needs to be well established in order to minimize systematics due to the extrapolation. Provided the temperature ratio and absolute temperatures are well known such a procedure does not introduce significant bias because the relative fluxes from the atmospheric models are much better constrained than the absolute fluxes. We add also that errors given on unreddened magnitudes in Table 3 do not account for possible systematic shifts on a level of 1% due to transformation of Tycho-2 and 2MASS magnitudes onto the Johnson photometric system.

3.8. Surface brightness

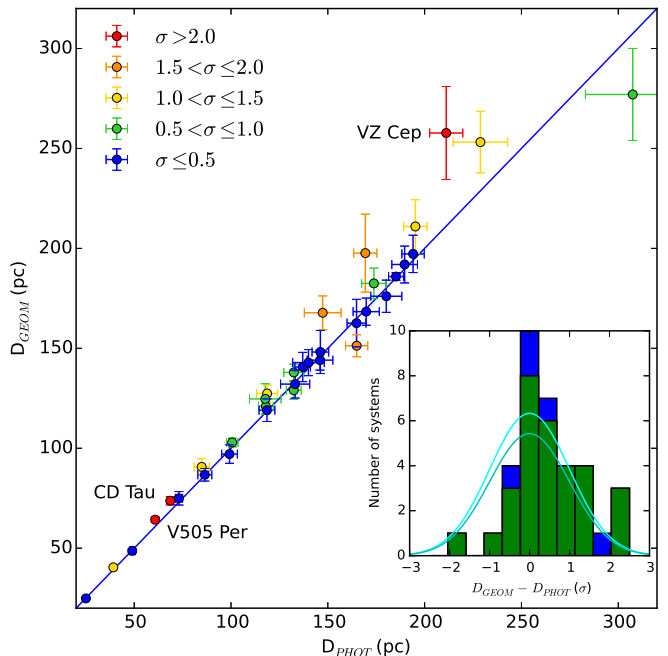


Figure 1. Comparison of geometric and photometric distances for all systems with deviation from a 1:1 relation expressed as fraction of σ and coded with color. Three named systems exhibit offsets larger than 2σ . Systems with $\sigma \leq 0.5$ define the best-fit subsample. *Inset:* the expected distribution of deviations from a 1:1 relation for all systems (upper line) and systems with the Gaia parallaxes (lower line) when random errors dominate. The histogram shows the actual distribution of deviations for the Gaia subsample (green) and the entire sample (green+blue).

We follow Hindsley & Bell (1989) to define the surface brightness parameter S :

$$S_i = m_{i,0} + 5 \log \phi, \quad (3)$$

where i denotes a particular band (B or V) and $m_{i,0}$ is the intrinsic magnitude in a given band. The surface brightness parameter S was then used to obtain the SBC relations by fitting it with first and fifth degree polynomials in a form:

$$S = \sum_{i=0}^{i=1,5} a_i X^i \quad (4)$$

where X is a given photometric color (see Sect. 4.3 for more details). Use of a higher order polynomial is justified by a strong non-linearity of the SBC relations for the blue-most colors (stellar spectral types earlier than A0).

4. RESULTS

4.1. Distances

Stassun & Torres (2016a,b) presented comprehensive comparisons of geometric distances from the Hipparcos and Gaia satellites with photometric distances derived from eclipsing binaries. We underline that we use here a different method to derive photometric distances, and our sample is significantly smaller but on other hand more carefully selected. Figure 1 shows the comparison of geometric and photometric distances, where difference between both distances is expressed in term of the standard deviation of distances σ . Inspection of the

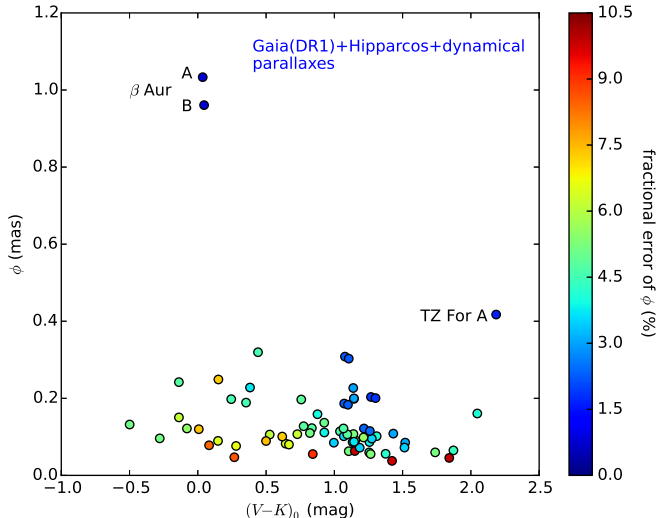


Figure 2. Geometric angular diameters of the eclipsing binary components and their uncertainties calculated from the most recent stellar radii and parallaxes. Three stars that are resolvable by interferometry are named.

figure confirms that detached eclipsing binary stars serve as almost perfect distance indicators, and the photometric distance is a very good proxy of true geometric distance, as long as issues with reddening and temperature are properly handled (e.g. see Section 4 in Torres et al. 2010). Both distances and their σ difference are given in Tab. 3.

The largest deviations from the 1:1 relation between geometric and photometric distance are for V505 Per (2.2σ), CD Tau (2.2σ) and VZ Cep (2.1σ). For the complete sample the reduced $\chi^2 = 0.99$ (34 degrees of freedom) i.e. it is fully consistent with statistical uncertainties dominating the error budget in the distance determination. However if we exclude the three most deviating systems the reduced $\chi^2 = 0.87$ (31 degrees of freedom) suggest that for the majority of systems the errors on the distance determinations are slightly overestimated. We note that the two strongly deviating systems (CD Tau and VZ Cep) also stand out in comparison of photometric and Hipparcos parallaxes (Stassun & Torres 2016a). A possible explanation is wrongly estimated temperatures or/and interstellar extinctions in case of those two systems or the presence of some additional systematics in trigonometric parallaxes. However more work is needed to figure out the source of the discrepancy.

The inset in Figure 1 shows histogram of deviations in terms of the σ from a sub-sample with Gaia parallaxes (30 systems, green) and from the rest of the sample (green+blue). Superimposed are the expected distributions of deviations when errors are uncorrelated and dominated by random uncertainties. We see a clear excess of systems with small deviations signifying that errors on distances are inflated both for the sample and the Gaia sub-sample. This is in agreement with the conclusion by Casertano et al. (2016). We see also that Gaia distances are on average larger than photometric distances, thus corroborating findings by Stassun & Torres (2016b).

4.2. Angular diameters

The distances were utilized to calculate geometric angular diameters for all the sample – see Tab. 4. Those angular diameters are direct limb darkened angular diameters and they are complimentary to angular diameters derived from interferometry (e.g. compilations by Boyajian et al. 2014; Challouf et al. 2014). They have an average precision of 4.7% limited by the precision of parallax determinations. The precision is better than 2% for 11 components. Figure 2 shows the derived angular diameters with uncertainties. One can note the clear dependency of uncertainty on angular size and color $(V - K)_0$, with bluer (hotter) stars having angular diameters more poorly determined. From all the sample only one star, the cooler component of TZ For, had its angular diameter measured directly with interferometry (Gallenne et al. 2016), however with much lower precision, and two components of β Aur were barely resolvable (Hummel et al. 1995).

4.3. SBC relations

Figure 3 shows the relation between the V-band surface brightness S_V and color $(V - K)_0$ against some interferometric SBC relations (Challouf et al. 2014; Boyajian et al. 2014; di Benedetto 2005; Kervella et al. 2004). Left and right panels correspond to S_V derived from the complete sample and the best-fit subsample, respectively. The best-fit systems were defined as those having their geometrical and photometric distances in agreement to better than 0.5σ – see Tab. 3 and Fig. 1. The V-band surface brightnesses derived from trigonometric parallaxes fits well on the Challouf et al. (2014) calibration with a spread of ~ 0.1 mag corresponding to 5% uncertainty in angular diameter, dominated by distance errors. The agreement with the interferometric relation is satisfactory, i.e. both methods of measuring angular diameters, direct from interferometry and semi-direct from eclipsing binary stars, show good consistency. The agreement is even better if we use the best-fit subsample.

In order to quantify the SBC relation we derived it directly. We fitted Eq. 4 to the S_V (see Sect. 3.8) using Orthogonal Distance Regression (Boggs & Rogers 1989) which accounts for the errors on the independent variable, in our case: color $(V - K)_0$. We fitted a fifth-order polynomial to all the data and a first order polynomial to the data from the best-fit systems. The results of the fitting are presented in Figure 4 and coefficients of the derived relations are given in Tab. 5. The precision of the SBC relation based on all systems is rather low ($\sim 5\%$) with the distance errors fully dominating the error budget. However, the use of systems having the best consistency of their geometric and photometric distances results in a remarkable improvement of the precision of the derived SBC relation by a factor of 2. The internal precision of the linear relation in predicting angular diameters of A-, F- and G-type stars is in fact comparable to or even better than published interferometric relations up-to-now, e.g.: Boyajian et al. (2014) – 4.6%, Challouf et al. (2014) – 3.7%, Kervella et al. (2004) – 2.8%⁴ and di Benedetto (2005) – 2.1%. The linear SBC relation we derived is almost indistinguishable from the

⁴ The precision of S_V - $(V - K)$ calibration by Kervella et al. (2004) is reported to be 1%. We recalculated the unweighted

Table 4
Metallicities from literature and derived quantities: masses, gravities and geometric angular diameters of all eclipsing binary components.

ID	[Fe/H]	Ref	Mass		Gravity		Angular Diameter	
			$M_1 \pm \sigma$ M_\odot	$M_2 \pm \sigma$ M_\odot	$\log g_1 \pm \sigma$ dex	$\log g_2 \pm \sigma$ dex	$\theta_1 \pm \sigma$ mas	$\theta_2 \pm \sigma$ mas
YZ Cas	0.10	1	2.263 ± 0.012	1.325 ± 0.007	3.988 ± 0.004	4.311 ± 0.005	0.242 ± 0.012	0.128 ± 0.006
AI Phe	-0.14	2	1.193 ± 0.004	1.242 ± 0.004	3.985 ± 0.008	3.605 ± 0.004	0.102 ± 0.004	0.161 ± 0.007
V505 Per	-0.12	3	1.272 ± 0.003	1.254 ± 0.003	4.323 ± 0.009	4.331 ± 0.010	0.186 ± 0.004	0.183 ± 0.004
AL Ari	-0.00	4	1.170 ± 0.006	0.916 ± 0.004	4.230 ± 0.004	4.489 ± 0.004	0.091 ± 0.005	0.060 ± 0.003
V570 Per	0.02	5	1.452 ± 0.009	1.352 ± 0.009	4.234 ± 0.017	4.283 ± 0.012	0.111 ± 0.004	0.101 ± 0.004
TZ For	0.02	6	1.957 ± 0.002	2.056 ± 0.002	3.532 ± 0.018	2.909 ± 0.011	0.199 ± 0.005	0.417 ± 0.007
V1229 Tau	0.06	7	2.203 ± 0.013	1.549 ± 0.010	4.306 ± 0.014	4.273 ± 0.026	0.122 ± 0.007	0.106 ± 0.006
V1094 Tau	-0.09	8	1.096 ± 0.004	1.012 ± 0.003	4.179 ± 0.004	4.355 ± 0.006	0.108 ± 0.003	0.085 ± 0.003
CD Tau	0.08	9	1.441 ± 0.016	1.367 ± 0.016	4.087 ± 0.010	4.174 ± 0.012	0.227 ± 0.007	0.200 ± 0.006
EW Ori	0.05	10	1.177 ± 0.009	1.130 ± 0.008	4.373 ± 0.005	4.409 ± 0.005	0.060 ± 0.003	0.056 ± 0.002
UX Men	0.04	11	1.229 ± 0.006	1.192 ± 0.007	4.270 ± 0.009	4.305 ± 0.009	0.122 ± 0.003	0.115 ± 0.003
TZ Men	-	-	2.482 ± 0.025	1.500 ± 0.010	4.224 ± 0.010	4.302 ± 0.010	0.150 ± 0.009	0.107 ± 0.007
beta Aur	0.15	12	2.365 ± 0.006	2.303 ± 0.006	3.929 ± 0.005	3.981 ± 0.005	1.033 ± 0.008	0.961 ± 0.008
RR Lyn	-0.24	13	1.922 ± 0.026	1.504 ± 0.041	3.900 ± 0.009	4.214 ± 0.020	0.320 ± 0.015	0.197 ± 0.010
WW Aur	-	-	1.964 ± 0.010	1.814 ± 0.008	4.161 ± 0.005	4.167 ± 0.006	0.198 ± 0.009	0.189 ± 0.009
HD71636	-0.05	14	1.512 ± 0.007	1.285 ± 0.006	4.226 ± 0.005	4.279 ± 0.005	0.123 ± 0.006	0.106 ± 0.005
VZ Hya	-0.20	15	1.271 ± 0.009	1.146 ± 0.006	4.305 ± 0.005	4.404 ± 0.006	0.085 ± 0.003	0.072 ± 0.003
KX Cnc	0.07	16	1.142 ± 0.003	1.132 ± 0.003	4.441 ± 0.002	4.450 ± 0.003	0.203 ± 0.004	0.201 ± 0.004
PT Vel	-	-	2.199 ± 0.016	1.626 ± 0.009	4.138 ± 0.009	4.264 ± 0.011	0.120 ± 0.009	0.089 ± 0.007
KW Hya	-	-	1.973 ± 0.036	1.485 ± 0.017	4.078 ± 0.010	4.269 ± 0.014	0.228 ± 0.008	0.159 ± 0.006
RZ Cha	-0.02	17	1.505 ± 0.027	1.513 ± 0.021	3.946 ± 0.011	3.893 ± 0.010	0.114 ± 0.005	0.122 ± 0.006
FM Leo	-	-	1.318 ± 0.011	1.287 ± 0.010	4.124 ± 0.023	4.189 ± 0.028	0.107 ± 0.006	0.098 ± 0.006
GG Lup	-0.10	18	4.079 ± 0.039	2.508 ± 0.022	4.295 ± 0.009	4.360 ± 0.009	0.132 ± 0.007	0.096 ± 0.005
V335 Ser	-	-	2.147 ± 0.014	1.905 ± 0.008	4.155 ± 0.011	4.240 ± 0.017	0.089 ± 0.006	0.076 ± 0.005
WZ Oph	-0.27	15	1.227 ± 0.007	1.220 ± 0.006	4.233 ± 0.008	4.220 ± 0.008	0.086 ± 0.003	0.087 ± 0.003
FL Lyr	-0.30	19	1.218 ± 0.016	0.958 ± 0.012	4.307 ± 0.021	4.453 ± 0.028	0.087 ± 0.003	0.065 ± 0.003
UZ Dra	-	-	1.306 ± 0.012	1.203 ± 0.011	4.330 ± 0.017	4.402 ± 0.019	0.063 ± 0.003	0.055 ± 0.003
V4089 Sgr	-	-	2.584 ± 0.012	1.607 ± 0.008	3.654 ± 0.005	4.233 ± 0.004	0.249 ± 0.018	0.101 ± 0.007
V1143 Cyg	0.08	20	1.356 ± 0.003	1.328 ± 0.002	4.317 ± 0.015	4.323 ± 0.015	0.308 ± 0.007	0.303 ± 0.007
MY Cyg	-	-	1.806 ± 0.025	1.782 ± 0.030	3.994 ± 0.020	4.013 ± 0.021	0.082 ± 0.005	0.080 ± 0.005
EI Cep	-0.04	21	1.772 ± 0.006	1.680 ± 0.006	3.762 ± 0.014	3.928 ± 0.016	0.137 ± 0.007	0.110 ± 0.006
VZ Cep	0.06	22	1.402 ± 0.015	1.108 ± 0.008	4.213 ± 0.008	4.446 ± 0.033	0.055 ± 0.005	0.038 ± 0.004
LL Aqr	0.02	23	1.195 ± 0.001	1.034 ± 0.001	4.272 ± 0.004	4.451 ± 0.004	0.095 ± 0.003	0.072 ± 0.003
EF Aqr	0.00	24	1.243 ± 0.006	0.946 ± 0.003	4.276 ± 0.007	4.447 ± 0.007	0.063 ± 0.006	0.045 ± 0.004
V821 Cas	-	-	2.088 ± 0.064	1.655 ± 0.050	4.024 ± 0.017	4.364 ± 0.024	0.078 ± 0.007	0.047 ± 0.004

Note. — References to metallicities: 1 - Pavlovski et al. (2014); 2 - Andersen et al. (1988); 3 - Tomasella et al. (2008a); 4 - Konorski et al. (2017); 5 - Tomasella et al. (2008b); 6 - Gallenne et al. (2016); 7 - Groenewegen et al. (2007); 8 - Maxted et al. (2015); 9 - Ribas et al. (1999); 10 - Clausen et al. (2010); 11 - Andersen et al. (1989); 12 - Southworth et al. (2007); 13 - Khaliullin et al. (2001); 14 - Holmberg et al. (2009); 15 - Clausen et al. (2008b); 16 - Sowell et al. (2012); 17 - Jørgensen & Gyldenkerne (1975); 18 - Andersen et al. (1993); 19 - Guillout et al. (2009); 20 - Andersen et al. (1987b); 21 - Torres et al. (2000); 22 - Torres & Lacy (2009); 23 - Graczyk et al. (2016); 24 - Vos et al. (2012)

Table 5
Coefficients of polynomial fits to the Surface Brightness parameter S in B - and V -bands.

Band	Color Index	N^a	Color Range (mag)	a_0	a_1	a_2	a_3	a_4	a_5	σ %
Linear fits (best-fit subsample)										
B	$(B-K)$	28	[-0.12:3.15]	2.640(18)	1.252(11)	-	-	-	-	2.5
V	$(B-K)$	28	[-0.12:3.15]	2.625(15)	0.959(9)	-	-	-	-	2.2
V	$(V-K)$	28	[-0.10:2.15]	2.644(19)	1.358(17)	-	-	-	-	2.7
Fifth-order polynomial fits (entire sample)										
B	$(B-K)$	70	[-0.7:3.15]	2.594(31)	1.423(88)	-0.592(164)	0.612(200)	-0.239(93)	0.031(14)	5.1
V	$(B-K)$	70	[-0.7:3.15]	2.579(27)	1.134(85)	-0.598(155)	0.623(187)	-0.245(87)	0.032(13)	5.0
V	$(V-K)$	70	[-0.5:2.15]	2.606(33)	1.526(134)	-0.989(317)	1.498(574)	-0.835(395)	0.156(88)	5.2

Note. — Notes. The S parameter is defined by the Equation 3. Colors are in the Johnson photometric system. The limb darkened stellar angular diameter is expressed in milliseconds of arc and follows from the equation: $\log \theta_{LD} = 0.2*(a_0 - m + a_1*X + \dots + a_5*X^5)$, where m is the observed extinction-free magnitude of a star in the B or V band and X is an extinction-free color. The last column gives the precision in predicting the angular diameter of stars in the given color range.

^a Number of stars used in the fit

relation by Boyajian et al. (2014), it compares well with the relation by Challouf et al. (2014), especially for the bluest colors, and also with di Benedetto (2005) for the reddest colors $(V-K)_0 > 1.0$. This is an important argument in favor of the eclipsing binary method as a fully independent way to derive the SBC calibration.

One of the advantages of using eclipsing binary stars comes from the very precise surface gravities derived for the individual components. This allows, in principle, to determine how a SBC relation might depend on surface gravity (Fig. 4). We see some hints of this dependence where higher surface gravities result in higher surface brightness but the spread is still large and it is premature to draw a conclusion here.

The broadband SBC relations calibrated onto a wide range of colors do not show any statistically significant metallicity dependence with an exception of the bluest colors (e.g. $(B-V)$, see Boyajian et al. 2014). We compiled the metallicity determinations for our sample from the literature (Tab. 4) in order to check the possible dependence. As expected, no clear metallicity dependence is visible for the $V-K$ color – see Figure 5, although the scatter may hide it.

For the SBC relation to be useful it should have small intrinsic scatter and be only weakly dependent on reddening. The SBC relation for the V band and $(V-K)$ has great potential in this respect. This relation is commonly used to predict angular diameters and to determine distances, e.g. to the Magellanic Clouds with accuracy of 2-3% (Pietrzyński et al. 2013; Graczyk et al. 2014). However, for early-type stars (O or B) the relation becomes non-negligibly inclined to the line of reddening and shows significantly larger scatter than for stars with spectral types later than A5 (e.g. Challouf et al. 2014). This reduces its potential for predicting angular diameters of early type stars. Kervella et al. (2004) reported that the SBC relations based on colors with a larger wavelength difference show smaller scatter, i.e. the colors $(B-K)$ and $(V-L)$. However their relations were constrained to intermediate- and late-type stars.

We decided to search for similar relations using our sample. We combined two surface brightness parameters (B - and V -band) with the six colors $(V-J)$, $(V-H)$, $(V-K)$, $(B-J)$, $(B-H)$ and $(B-K)$. We fit the surface brightness parameters for the best-fit and all systems using first- and fifth-order polynomials, respectively. Figure 6 shows the two derived promising SBC relations based on $(B-K)$ color and with the rms minimized. The appropriate polynomial coefficients and the precision of angular diameter prediction are reported in Tab. 5. Both relations give precisions in the predicted angular diameters of 5% for the entire sample, 2-3% for the best-fit subsample, and have the smallest inclination of the relations to the reddening line for bluest colors. We note here that the real precision is lower because of the global systematic uncertainty of Gaia DR1 parallaxes. We estimated that the an upper limit of the systematics is about 3% for our systems.

5. DISCUSSION

The main purpose of the paper is to show that the inverse eclipsing binary method allows for independent and precise calibration of the SBC relations. Results presented in Section 4.3 fully corroborate this premise. Still,

the precision of the derived relations is not significantly better than those derived from interferometric measurements of stellar angular diameters. In this section we are going to quantify the necessary steps in order to reach sub-percent precision in predicting angular diameters.

5.1. Uniform analysis

We compiled in this work data from numerous papers published by many different groups of researchers. Each group uses different quality photometric and spectroscopic data, different methodology to derive radial velocities, analysis of light and radial velocity curves (separated, simultaneous, single light curve, multi-band light curves), different ways of deriving effective temperatures (color-temperature calibrations, atmospheric model analysis) and finally different sets of astrophysical numerical constants. During this work we made some effort to homogenize existing data on eclipsing binary stars, but it was constrained to the effective temperatures, their ratio and the radial velocity semi-amplitudes.

However, to pin-down systematics a full homogenous re-analysis of each system would be needed using the same methodology and software, and also similar quality observables. That would result in better evaluation of relative precision of each data sets and it would augmented the internal precision of the physical parameters of the whole sample. Significant help in this respect can be expected from using new, high precision numerical codes like *ellc* (Maxted 2016) or *Phoebe-2* (Prša et al. 2016), allowing for a very homogenous analysis of the full sample.

Ideally uniform space-based high-precision medium-cadence photometry and homogenous high-resolution, high-stability spectroscopic ground-based data for all the sample would suit best the purpose of the very precise SBC calibration. Such light curves will become available for many of the systems here if the TESS mission is successfully launched. We see this as a long-future next, natural step resulting in additional improvements over internal consistency and precision of derived physical parameters.

5.2. Sample enlargement

In order to increase the number of eclipsing binaries with suitable data for this programme, we have selected a number of additional, suitable detached eclipsing binary systems and have collected spectroscopic and photometric data for them. They cover a wide range of spectral classes from B- to early K-type and they are mostly within 300 pc from the Sun (low extinction regime). Besides AL Ari, for which we are already presenting derived physical parameters and a paper describing full analysis will be published soon (Konorski et al. 2017) our ongoing analysis is at an advanced stage for about 20 more systems.

The sample will be expanded in the near future with systems having more precise Gaia parallaxes within and beyond 300 pc horizon. More systems will also join the sample from efforts of other research groups investigating eclipsing binary stars as a large number of high quality light curves from ground based surveys (e.g. Super-WASP, soon the LSST) and space based surveys (e.g. Kepler-2, soon TESS) is registered for both known and

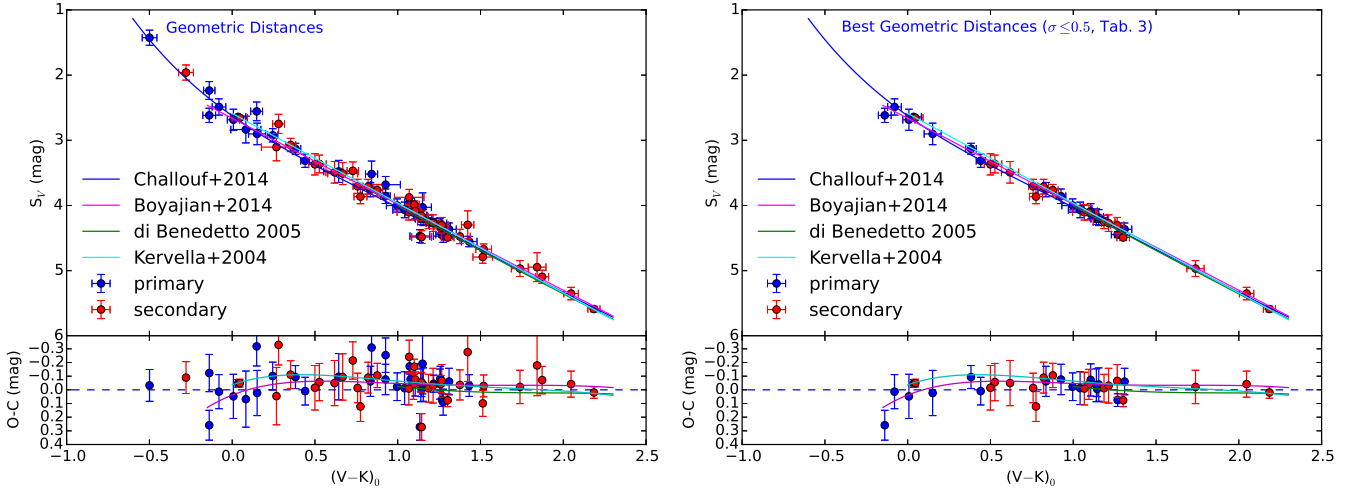


Figure 3. V -band surface brightness vs Johnson color $V-K$ relation. *Left panel:* for all stars based on their geometric distances. *Right panel:* for 14 systems with best agreement between the geometric and the photometric distances. Continuous lines correspond to several published interferometric SBC relations. Lower panels show O-C residuals calculated with respect to SBC relation by Challouf et al. (2014) - dashed line.

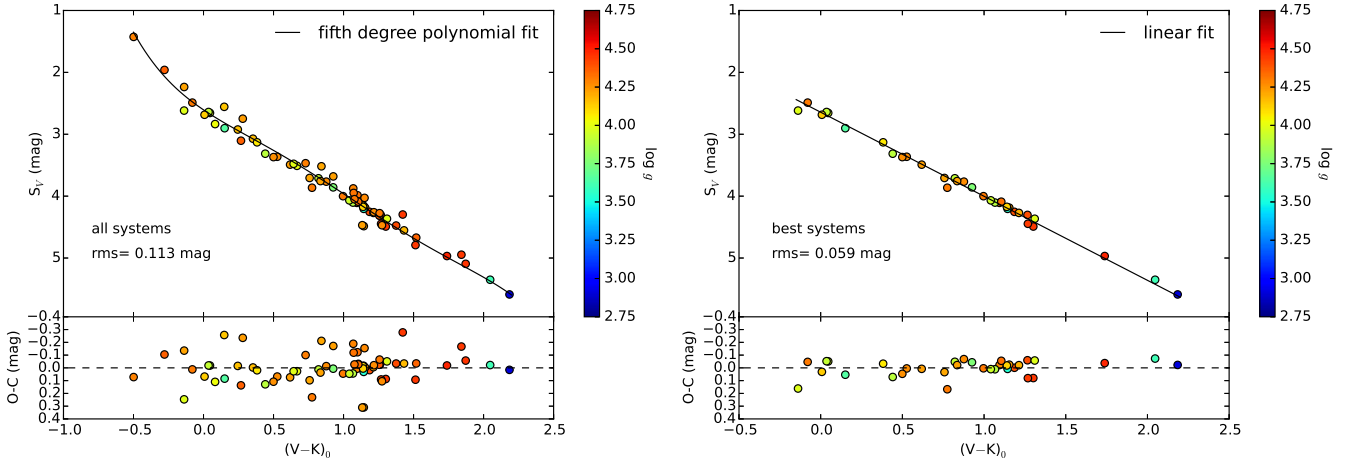


Figure 4. V -band surface brightness vs Johnson color $V-K$ relation with the addition of the surface gravity color scale (right vertical axis). *Left panel:* all the systems. *Right panel:* the systems with the best-fit distances.

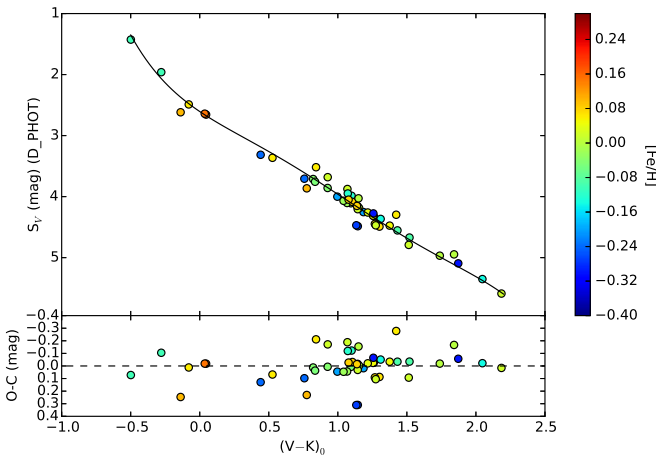


Figure 5. V -band surface brightness vs Johnson color $V-K$ for systems with determined metallicity. The continuous line represents a fifth-order polynomial fit to the entire sample.

newly discovered systems. Those efforts will surely result in enlarging significantly the sample to about 100 systems covering B-, A-, F- and G-type stars. More systems will not only help to reduce statistical errors of relations but also to determine the intrinsic spread of the SBC relations.

5.3. Parallaxes

Future more precise Gaia parallaxes are fundamental for any significant improvement to SBC relations presented here. We forecast expected precision of Gaia parallaxes for the sample as follows. We assumed conservatively that the precision of astrometry for bright stars ($3 \text{ mag} < G < 12 \text{ mag}$) will be $15 \mu\text{as}$ and that the photocenter movement of an eclipsing binary will be unequivocally detected and taken into account when it is larger than $35 \mu\text{as}$. The resulting expected mean relative precision of Gaia parallaxes will be 0.6% for our sample. Systematic uncertainty introduced into the prediction of angular diameters will likely be smaller but to be conclusive on this point we need to wait for a final

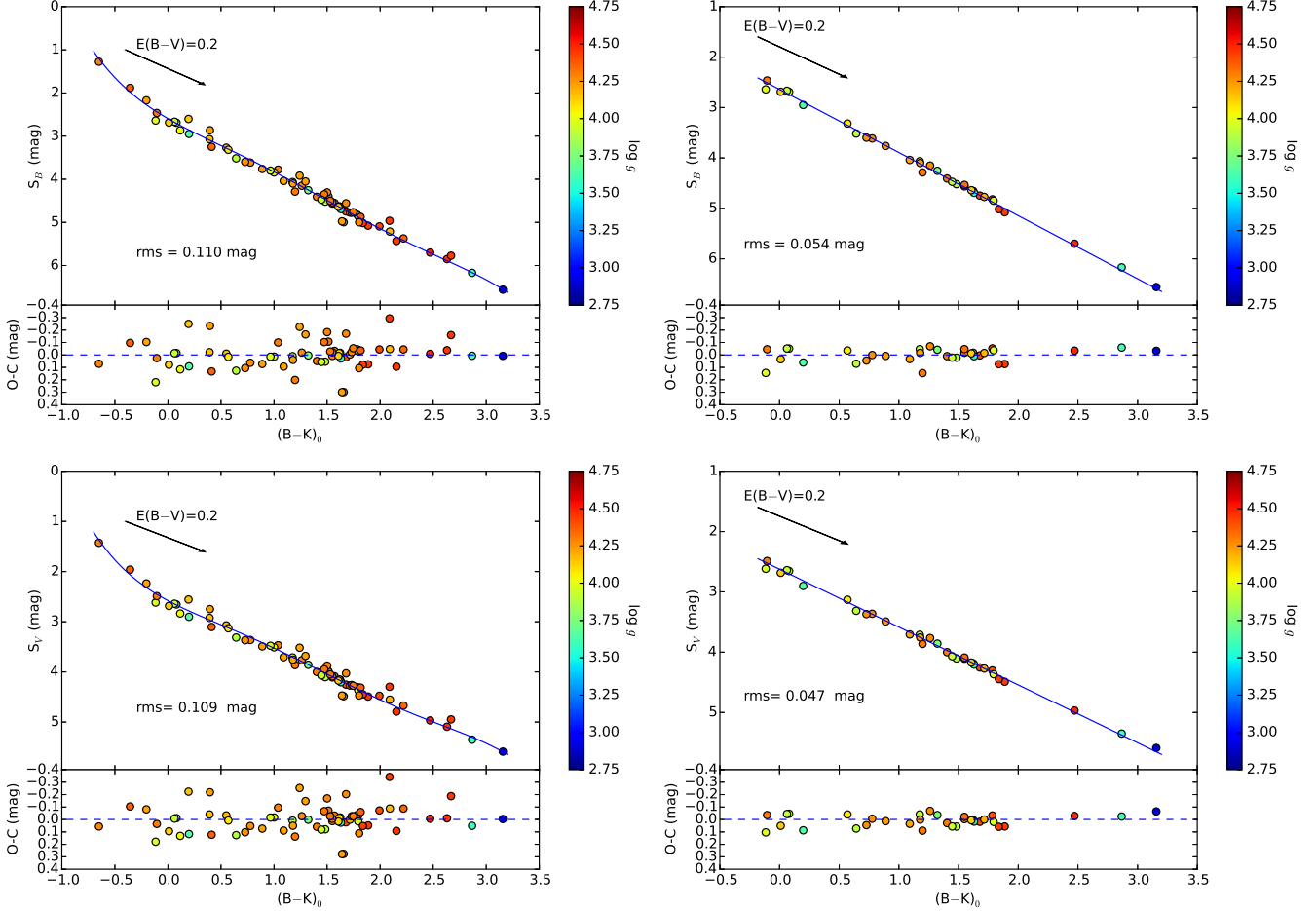


Figure 6. Surface brightness vs Johnson color $B-K$ relations. *Upper panel:* calibrated for the B band. *Lower panel:* calibrated for the V band. The continuous line in the left panels shows fifth-order polynomial fits to all stars in the sample, and in the right panels the line shows linear fits to the best-fit subsample. The reddening vector is denoted as an arrow. The root mean square of the relations is given. The surface gravity in cgs units is color coded.

Gaia release quality evaluation. Figure 7 presents the expected angular diameters of stars in our sample after the final Gaia data release, assuming the same radii and uncertainties as in Tab. 3. Inspection of this figure suggests that much improvement is expected, especially for blue stars. Angular diameters with a sub-percent precision will be available for more than half of all components in our eclipsing binary sample. We add that the sample will be augmented by very precise dynamical parallaxes from interferometric orbits for a number of long period eclipsing binary stars.

5.4. Disentangling of component magnitudes

It is interesting to estimate to what extent our extrapolation procedure introduce a bias. As was mentioned already in Sec. 3.7, flux ratios are calculated using precomputed intensities based on ATLAS9 atmosphere models which assume a plane-parallel geometry and local thermodynamic equilibrium (LTE). When components have similar effective temperatures to within about 100 K their light ratio changes very little over the optical and NIR range of the spectrum and, regardless of the adopted model atmosphere, the extrapolation leads to negligible errors in comparison with observational photo-

metric uncertainties. However the situation is somewhat different when the temperature difference between the components is much larger, say of the order of 1000 K.

For A-, F- and G-type stars with given atmospheric parameters (T_{eff} , $\log g$, $[\text{Fe}/\text{H}]$) and solar-like compositions their absolute spectral energy distributions predicted by various atmospheric models (plane parallel, spherical, LTE and non-LTE) in a range of B and K bands have differences between them of up to 5%, but significantly smaller regarding relative fluxes (i.e. colors) (e.g. Bessell et al. 1998; Martins & Coelho 2007; Edvardsson 2008; Plez 2011). Comparison of model fluxes with empirical fluxes in the aforementioned range of the spectrum gives also very good agreements. As a result, we can expect, on average, a small systematic uncertainty in the derived colors (reaching up to 0.02 mag) even in cases of larger temperature difference between the components. Such an error would be only a fraction of the typical uncertainty of an intrinsic color. This uncertainty can be mitigated even further by using multi-band photometry and carefully determined temperatures derived from disentangled spectra. For hotter stars (O- and B-type) use of plane-parallel and LTE models may lead to much larger systematic shifts (e.g. Aufdenberg et al.

1998; Cugier 2012), however these issues will be addressed in a forthcoming paper.

5.5. *Photometry and transformations into standard system*

5.5.1. *Optical*

The precision of transformation between the Tycho-2 and Johnson photometric systems is about 1% (Bessell 2000) resulting in additional systematic uncertainty in our SBC relations. To mitigate the problem one would use original Tycho-2 B_T and V_T magnitudes and to express the calibration in this system. However we notice that for a few systems in our sample (EW Ori, VZ Hya, VZ Cep, LL Aqr and EF Aqr), Tycho-2 photometry transformed into B, V magnitudes give optical and NIR colors which are inconsistent with each other and with temperatures of the stars. In those cases we used other sources of V -band magnitudes. The source of discrepancy is unclear to us, but we think that although the Tycho-2 photometry is multi-epoch in particular cases mean B_T and V_T magnitudes are affected by the presence of eclipses and/or other kind of systematics (e.g. transformation errors). That strengthens the case for well-calibrated, precise and uniform optical B, V photometry in the standard Johnson system for stars in the sample. In the optical, provided that a photometric system is close to the standard one, it is expected that transformation from instrumental system to the standard one would not produce systematic errors larger than 0.5%.

5.5.2. *NIR*

For the overwhelming majority of eclipsing binary systems, well calibrated photometry NIR comes only from the single-epoch 2MASS survey. We transformed 2MASS magnitudes into the Johnson system which may introduce systematics of up to 1% (0.02 mag), because of poor definition of the Johnson system in NIR. As an example of this fact the transformation equation for $(V-K)$ color used by Holmberg et al. (2007) has an offset of -0.02 mag with respect to the transformation equation we used, of course a non-negligible value when we deal with sub-percent precision. Preferentially the future SBC calibration should be expressed in the 2MASS photometric system which is well calibrated (e.g. Cohen et al. 2003) and it is based on all-sky network of standard stars, or eventually by using other NIR system which have similar bandpasses and precisely determined transformation (e.g. SAAO).

Single-epoch photometry is prone to some accidental errors and the statistical uncertainty of one measurement is relatively large. Because of that it would be advisable to carry out new, high quality multi epoch NIR photometry secured for stars in the sample. It would significantly help in reducing statistical uncertainties and in removing any accidental photometric errors. We already started a campaign to secure NIR photometry for southern and equatorial stars from the sample with the plan to derive precise out-of-eclipse magnitudes and later also to provide full NIR light curves for some eclipsing binaries, especially those having large effective temperature difference between components.

5.6. *Quantifying error contributions*

- **Radii:** the mean precision of stellar radii determination in our sample is 1.2%. By using about 100 systems it would be possible to pin-down the statistical error by a factor of 10, i.e. to 0.1-0.2%. Systematics will come mostly from the numerical tools for the analysis of eclipsing binary stars, and it is expected to be of order of 0.1%.
- **Parallaxes:** taking into account the photocenter movements of the eclipsing binaries, the mean expected precision of Gaia parallaxes would be 0.6%. The systematic error is expected to be significantly smaller.
- **Disentangling of magnitudes:** up to 0.01 mag of systematics in derived colors and magnitudes translates into a 0.3% mean systematic uncertainty in predicting angular diameters. However, by if we were to use full NIR light curves and/or by using equal-temperature systems, then this error could be almost eliminated because it would be possible to determine the NIR magnitudes directly.
- **Photometric zero-points and transformations:** in best cases of well-defined photometric systems (Section 5.5) we expect 0.7% systematics in colors and magnitudes.
- **Interstellar extinction:**
 - a) **Total extinction:** the reddening is low for almost all our systems. When we assume a standard Galactic extinction curve with $R_V = 3.1$, it introduces only a little additional uncertainty of about 0.03 mag in the $(V-K)_0$ color. Because the reddening line is largely parallel to the SBC relation, this translates into only a 0.006 mag statistical uncertainty (0.3 %) in predicting the angular diameter.
 - b) **Reddening law:** for about 25% of stars in within 1kpc from the sun (e.g. Fitzpatrick & Masana 2007; Krelowski & Strobel 2012), we expect deviations from the universal law. R_V can vary significantly, but mostly lies between 2.7 and 3.7 (e.g. Gontcharov 2012). When this is not accounted for, it shows as an additional intrinsic scatter in the SBC relation that amounts to about 0.02 mag in some individual cases.

The statistical uncertainty of the future SBC relation is expected to be well below 1% provided the number of suitable systems is sufficient (about 100 systems) and the internal dispersion of a given relation is low. By combining all conservative estimates of errors from the above considerations in quadrature we obtain an upper limit of 0.9% on the systematic uncertainty. This error is dominated by the photometric uncertainties.

6. FINAL REMARKS

New Gaia parallaxes combined with Hipparcos and dynamical parallaxes allow us to derive for the first time the SBC relations based fully on the eclipsing binary stars. The precision of the derived relations for A-, F-, and G-type stars is comparable to the precision of relations derived from interferometric angular diameters, and both types of relations are mutually consistent. The eclipsing binary method has no serious limitations if it based

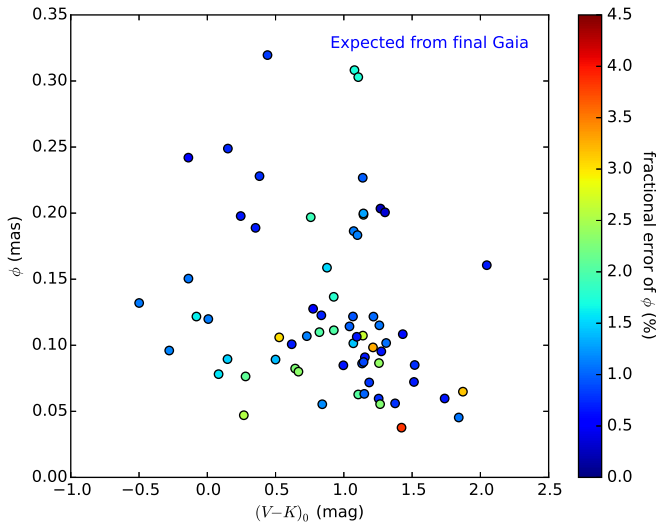


Figure 7. Predicted angular diameter uncertainties for stars in our sample after the final Gaia release. Note the change in scale of the color bar with respect to Fig. 2. The error-bars would be in most cases smaller than the size of the circles.

on a well-selected sample of eclipsing binaries, a self-consistent analysis method, and proper sanity checks. To expand the SBC relation to O- and B-type stars we propose to use the $B-K$ color, which allows reducing interstellar extinction uncertainties. We also discussed all the steps necessary to obtain precise and accurate SBC relations that allow for a precision better than 1% of the angular diameter predictions in the future.

The research leading to these results has received funding from the European Research Council (ERC) under the European Union’s Horizon 2020 research and innovation program (grant agreement No 695099).

We are grateful for financial support from Polish National Science Center grant MAESTRO 2012/06/A/ST9/00269. Support from the BASAL Centro de Astrofísica y Tecnologías Afines (CATA) PFB-06/2007, the Millenium Institute of Astrophysics (MAS) of the Iniciativa Científica Milenio del Ministerio de Economía, Fomento y Turismo de Chile, project IC120009 and the IdP II 2015 0002 64 grant of the Polish Ministry of Science and Higher Education is also acknowledged. We are also thanks to the staffs in La Silla Observatory (ESO) and Las Campanas Observatory (Carnegie) for their excellent support.

We also thank the anonymous referee for remarks and corrections to the text.

This research has made extensive use of the excellent astronomical SIMBAD database and of the VizieR catalogue access tool, operated at CDS, Strasbourg, France and made also use of NASA’s Astrophysics Data System Bibliographic Services (ADS).

This publication makes use of data products from the Two Micron All Sky Survey, which is a joint project of the University of Massachusetts and the Infrared Processing and Analysis Center/California Institute of Technology, funded by the National Aeronautics and Space Administration and the National Science Foundation.

We dedicate this work to Prof. Bohdan Paczyński who

encouraged us many years ago to work on this subject.

REFERENCES

- Abt, H. A., & Levato, H. 1978, *PASP*, 90, 201
- Albrecht, S., Reffert, S., Snellen, I., Quirrenbach, A., & Mitchell, D. S. 2007, *A&A*, 474, 565
- Alonso, A., Arribas, S., & Martínez-Roger, C. 1996, *A&A*, 313, 873
- Ammons, S. M., Robinson, S. E., Strader, J., et al. 2006, *ApJ*, 638, 1004
- Andersen, J., Gjerløff, H., & Imbert, M. 1975, *A&A*, 44, 349
- Andersen, J., & Vaz, L. P. R. 1984, *A&A*, 130, 102
- Andersen, J., Clausen, J. V., & Nordström, B. 1987a, *A&A*, 175, 60
- Andersen, J., García, J. M., Giménez, A., & Nordström, B. 1987b, *A&A*, 174, 107
- Andersen, J., Clausen, C. V., Gustafsson, B., Nordström, B., & VandenBerg, D. A., 1988, *A&A*, 196, 128
- Andersen, J., Clausen, J. V., & Magain, P. 1989, *A&A*, 211, 346
- Andersen, J. 1991, *A&A Rev.*, 3, 91
- Andersen, J., Clausen, J. V., Nordström, B., Tomkin, J., & Mayor, M. 1991, *A&A*, 246, 99
- Andersen, J., Clausen, J. V., & Giménez, A. 1993, *A&A*, 277, 439
- Aufdenberg, J. P., Hauschildt, P. H., & Baron, E. 1998, *ASP Conf. Series*, Vol. 131, 127
- Bailer-Jones, C. A. L. 2015, *PASP*, 127, 994
- Bakiş, V., Bakiş, H., Demircan, O., & Eker, Z. 2008, *MNRAS*, 384, 1657
- Barnes, T. G., Evans, D. S., & Moffett, T. J. 1978, *MNRAS*, 183, 285
- Batten, A. H., Fletcher, J. M., & Mann, P. J. 1978, *Publ. Dom. Astrophys. Obs.*, Victoria, 15, 121
- Behr, B. B., Cenko, A. T., Hajian, A. R., et al. 2011, *AJ*, 142, 6
- Bessell, M. S., Brett J. M., 1988, *PASP*, 100, 1134
- Bessell, M. S., Castelli, F., & Plez, B. 1998, *A&A*, 333, 231
- Bessell, M. 2000, *PASP*, 112, 961
- Bilir, S., Ak, T., Soydugan, E., et al. 2008, *Astron. Nachr.*, 117, 393
- Boggs, P. T., & Rogers, J. E. 1989, *Orthogonal Distance Regression*, National Institute of Standards and Technology, Gaithersburg, Maryland, Internal Report 89-4197 (Revised 1990)
- Bonneau, D., Clausse, J.-M., Delfosse, X., et al. 2006, *A&A*, 456, 789
- Boyajian, T. S., van Belle, G., & von Braun, K. 2014, *AJ*, 147, 47
- Budding, E., Butland, R., & Blackford, M. 2015, *MNRAS*, 448, 3784
- Çakirli, Ö., Ibañoğlu, C., Bilir, S., & Sipahi, E. 2009, *MNRAS*, 395, 1649
- Cannon, A. J., & Pickering, E. C. 1919, *The Henry Draper Catalogue*, Cambridge, Ann. Astron. Obs. Harvard College, Vol. 93
- Carpenter J. M., 2001, *AJ*, 121, 2851
- Casagrande, L., I. Ramírez, I., Meléndez, J., Bessell, M., & Asplund, M. 2010, *A&A*, 512, 54
- Casertano, S., Riess, A. G., Bucciarelli, B., & Lattanzi, M. G. 2016, arXiv:1609.05175v1
- Challouf, M., Nardetto, N., Mourard, D., et al., 2014, *A&A*, 570, 104
- Clausen, J. V., & Grønbech, B. 1976, *A&A*, 48, 49
- Clausen, J. V., Vaz, L. P. R., García, J. M., et al. 2008a, *A&A*, 487, 1081
- Clausen, J. V., Torres, G., Bruntt, H., et al. 2008b, *A&A*, 487, 1095
- Clausen, J. V., Bruntt, H., Olsen, E. H., Helt, B. E., & Claret, A., 2010, *A&A*, 511, 22
- Cohen, M., Wheaton, Wm., A., & Megeath, S. T. 2003, *AJ*, 126, 1090
- Cugier, H. 2012, *A&A*, 547, 42
- David, T. J., Conroy, K. E., Hillenbrand, L. A., et al. 2016, *AJ*, 151, 112
- de Bruijne, J. H. J., Rygl, K. L. J., & Antoja, T., 2014, *The Milky Way Unravalled by Gaia: GREAT Science from the Gaia Data Releases*, EAS Publications Series 67-68, N.A. Walton, F. Figueras, L. Balaguer-Nunez and C. Soubiran, 23
- Di Benedetto, G. P. 2005, *MNRAS*, 357, 174
- Ducati, J. R. 2002, *VizieR Online Data Catalog*: 2237, 0
- Edvardsson, B. 2008, *PhST*, Vol. 133, 4011
- Eker, Z., Bilir, S., Soydugan, F., et al. 2014, *PASA*, 31, 24
- Fitzpatrick, E. L., & Massa, D. 2007, *ApJ*, 663, 320
- Flower, P. J. 1996, *ApJ*, 469, 355
- Fouqué, P., & Gieren, W. 1997, *A&A*, 320, 799
- Gaia Collaboration: Brown, A. G. A., Vallenari, A., Prusti, T., de Bruijne, J., Mignard, F., et al. 2016, arXiv:1609.04172v1
- Gallenne, A., Pietrzyński, G., Graczyk, D., et al. 2016, *A&A*, 586, 35

- Gieren, W., Storm, J., Barnes, T. G., et al. 1995, *ApJ*, 627, 224
- Giménez, A., & Margrave, T. E. 1985, *AJ*, 90, 358
- Giuricin, G., Mardirossian, F., Mezzetti, M., & Predolin, F. 1980, *A&A*, 85, 259
- Gontcharov, G. A. 2012, *AstL*, 38, 12
- González Hernández, J. I. & Bonifacio, P. 2009, *A&A*, 497, 497
- Graczyk, D., Pietrzyński, G., Thompson, I. B., et al., 2014, *ApJ*, 780, 59
- Graczyk, D., Maxted, P. F. L., Pietrzyński, G., et al. 2015, *A&A*, 581, 106
- Graczyk, D., Smolec, R., Pavlovski, K., et al. 2016, *A&A*, 594, 92
- Griffin, R. F. 2013, *Observatory*, 133, 156
- Groenewegen, M. A. T., Decin, L., Salaris, M., & De Cat, P. 2007, *A&A*, 463, 579
- Guillout, P., Klutsch, A., Frasca, A., et al. 2009, *A&A*, 504, 829
- Gülmen, O., Güdür, N., Sezer, C., 1986, *IBVS*, 2953, 1
- Habbereiter, M., Schmutz, W., Kosovichev, A. G. 2008, *ApJ*, 675, 53
- Helminiak, K. G., Konacki, M., Ratajczak, M., & Muterspaugh M. W., 2009, *MNRAS*, 400, 969
- Henry, G. W., Fekel, F. C., Sowell, J. R., & Gearhart, J. S. 2006, *AJ*, 132, 2489
- Hill, G., Hilditch, R. W., Younger, F., & Fisher, W. A. 1975, *MmRAS*, 79, 131
- Hindsley, R. B., & Bell, R. A. 1989, *ApJ*, 341, 1004
- Holmberg, J., Nordström, B., & Andersen, J. 2007, *A&A*, 475, 519
- Holmberg, J., Nordström, B., & Andersen, J. 2009, *A&A*, 501, 941
- Houdashelt, M. L., Bell, R. A., & Sweigart, A. V. 2000, *AJ*, 119, 1448
- Houk, N., & Cowley, A. P. 1975, *Michigan Spectral Catalog*, Vol. 1, Univ. of Michigan, Ann Arbor, USA
- Houk, N. 1978, *Michigan Catalogue of two-dimensional spectral types for HD stars*, Vol. 2, Univ. of Michigan, Ann Arbor
- Houk, N., & Swift, C. 1999, *Michigan Catalogue of two-dimensional spectral types for HD stars*, Vol. 5, Univ. of Michigan, Ann Arbor
- Høg, E., Fabricius, C., Makarov, V. V., et al. 2000, *A&A*, 357, 367
- Hrivnak, B. J., & Milone, E. F. 1984, *ApJ*, 282, 748
- Hummel, C. A., Armstrong, J. T., Buscher, D. F., et al. 1995, *AJ*, 110, 376
- Imbert, M. 1986, *A&AS*, 65, 97
- Imbert, M. 2002, *A&A*, 387, 850
- Jerzykiewicz, M. 2001, *Acta Astron.*, 51, 151
- Jørgensen, H. E., & Gyldenkerne, K. 1975, *A&A*, 44, 343
- Kervella, P., Thévenin, F., Di Folco, E., Ségransan, D., 2004, *A&A*, 426, 297
- Khaliullin, Kh. F., Khaliullina, A. I., & Krylov, A. V. 2001, *Astron. Rep.*, 45, 888
- Khaliullin, Kh. F., & Khaliullina, A. I. 2002, *Astron. Rep.*, 46, 119
- Kiyokawa, M., & Kitamura, M. 1975, *Ann. Tokyo Astron. Obs.*, second series, 15, 117
- Kirkby-Knet, J. A., Maxted, P. F. L., Serenelli, A. M., et al., 2016, *A&A*, 591, 124
- Konorski, P., Graczyk, D., Pietrzyński, G., et al. 2017, in preparation
- Krelowski, J. & Strobel, A. 2012, *AN*, 333, 60
- Kruszewski, A., & Semeniuk, I., 1999, *AcA*, 49, 561
- Kurucz R., 1993, *ATLAS9 Stellar Atmosphere Programs and 2 km s⁻¹ Grid*, (Cambridge, MA: SAO) Kurucz CD-ROM No. 13,
- Lacy, C. H. S. 1977, *ApJ*, 213, 458
- Lacy, C. H. S. 1981, *ApJ*, 251, 591
- Lacy, C. H., Gülmen, O., Güdür, N., Sezer, C., 1989, *AJ*, 97, 822
- Lacy, C. H. S., 2002, *AJ*, 124, 1162
- Lacy, C. H. S., Fekel, F. C., & Claret, A., 2012, *AJ*, 144, 63
- Lutz, T. E., & Kelker, D. H. 1973, *PASP*, 85, 573
- Lyubimkov, L. S., Rachkovskaya, T. M., & Rostopchin, S. I. 1996, *Astron. Rep.*, 40, 802
- Malkov, O. Y., 1993, *Bull. Inform. Centr. Donn. Strasb.*, 42, 27
- Martins, L. P., & Coelho, P. 2007, *MNRAS*, 381, 1329
- Masana, E., Jordi, C., & Ribas, I. 2006, *A&A*, 450, 735
- Maxted, P. F. L., Hutcheon, R. J., Torres, G., et al. 2015, *A&A*, 578, 25
- Maxted, P. F. L. 2016, *A&A*, 591, 111
- Mermilliod, J. C. 1991, *Catalogue of Homogeneous Means in the UVB System*, Institut d'Astronomie, Université de Lausanne, Geneva
- Munari, U., Dallaporta, S., Siviero, A., et al. 2004, *A&A*, 418, L31
- Napiwotzki, R., Schoenberner, D., Wenske, V. 1993, *A&A*, 268, 653
- Nesterov, V. V., Kuzmin, A. V., Ashimbaeva, N. T., et al., 1995, *A&AS*, 110, 367
- Nordström, B., & Johansen, K. T. 1994b, *A&A*, 291, 777
- Ochsenbein, F., Bauer, P. & Marcout, J. 2000, *A&AS*, 143, 23
- Olsen, E. H. 1983, *A&AS*, 54, 55
- Pavlovski, K., Tamajo, E., Koubský, et al. 2009, *MNRAS*, 400, 791
- Pavlovski, K., Southworth, J., Kolbas, V., & Smalley, B. 2014, *MNRAS*, 438, 590
- Pecaut, M. J., & Mamajek, E. E. 2013, *ApJS*, 208, 9
- Pietrzyński, G., Graczyk, D., Gieren, W., et al., 2013, *Nature*, 495, 76
- Pitjeva, E. V., & Standish, E. M. 2009, *Celest. Mech. Dyn. Astr.*, 103, 356
- Plez, B. 2011, *JPhCD*, Vol. 328, 2005
- Popper, D. M. 1965, *ApJ*, 141, 126
- Popper, D. M. 1966, *AJ*, 71, 175
- Popper, D. M. 1971, *ApJ*, 169, 549
- Popper, D. M. 1980, *ARA&A*, 18, 115
- Popper, D. M., & Etzel, P. B. 1981, *AJ*, 86, 102
- Popper, D. M. 1984, *AJ*, 89, 132
- Popper, D. M., Lacy, C. H., Frueh, M. L., & Turner, A. E. 1986, *AJ*, 91, 383
- Popper, D. M. 1998, *PASP*, 110, 919
- Prša, A., Conroy, K. E., Horvat, M., et al. 2016, *ApJS*, 227, 29
- Ratajczak, M., Kwiatkowski, T., Schwarzenberg-Czerny, A., et al. 2010, *MNRAS*, 402, 2424
- Ramírez, I., & Meléndez, J. 2005, *AJ*, 626, 465
- Ribas, I., Jordi, C., & Jordi, T. 1999, *MNRAS*, 309, 199
- Sandage, A., & Saha, A. 2002, *AJ*, 123, 2047
- Schlegel, D. J., Finkbeiner, D. P. & Davis, M., 1998, *ApJ*, 500, 525
- Semeniuk, I. 2001, *AcA*, 51, 75
- Skrutskie, M. F., Cutri, R. M., Stiening, R., et al. 2006, *AJ*, 131, 1163
- Smalley, B., Gardiner, R. B., Kupka, F., Bessell, M. F. 2002, *A&A*, 395, 601
- Smith, B. 1948, *ApJ*, 108, 504
- Southworth, J., Smalley, B., Maxted, P. F. L., Claret, A., & Etzel, P. B. 2005, *MNRAS*, 363, 529
- Southworth, J., Bruntt, H., & Buzasi, D. L. 2007, *A&A*, 467, 1215
- Southworth, J. 2013, *A&A*, 557, 119
- Southworth, J. 2015, *Living Together: Planets, Host Stars and Binaries*, ASP Conference Series 496, S. Rucinski, G. Torres, and M. Zejda, San Francisco: Astronomical Society of the Pacific, 164
- Sowell, J. R., Henry, G. W., & Fekel, F. C. 2012, *AJ*, 143, 5
- Stassun, K. G., & Torres, G. 2016, *AJ*, 152, 180
- Stassun, K. G., & Torres, G. 2016, *ApJ*, 831L, 6
- Storm, J., Gieren, W., Fouqué, P., et al. 2011, *A&A*, 534, 94
- Suchomska, K., Graczyk, D., Smolec, R., et al. 2015, *MNRAS*, 451, 91
- Tomasella, L., Munari, U., Siviero, A. et al. 2008a, *A&A*, 480, 465
- Tomasella, L., Munari, U., Cassisi, S., et al. 2008b, *A&A*, 483, 263
- Tomkin, J., & Fekel, F. C. 2006, *AJ*, 131, 2652
- Torres, G., & Lacy, C. H. S. 2009, *AJ*, 137, 507
- Torres, G., Andersen, J., Nordström, B., & Latham, D. W. 2000, *AJ*, 119, 1942
- Torres, G., Andersen, J., & Giménez, A. 2010, *A&A Rev.*, 18, 67
- Tucker, R. S., Sowell, J. R., Williamon, R. M., & Coughlin, J. L., 2009, *AJ*, 137, 2949
- van Hamme, W., & Wilson, R. E. 2007, *ApJ*, 661, 1129
- van Leeuwen, F. 2007, *A&A*, 474, 653
- Veramendi, M. E., & González, J. F. 2015, *New Astronomy*, 34, 266
- Vos J., Clausen, J. V., Jørgensen, U. G., et al. 2012, *A&A*, 540, 64
- Wenger, M., Ochsenbein, F., Egret, D., et al. 2000, *A&AS*, 143, 9
- Wilson, R. E., & Devinney, E. J. 1971, *ApJ*, 166, 605
- Wilson, R. E. 1979, *ApJ*, 234, 1054
- Wilson, R. E. 1990, *ApJ*, 356, 613
- Wilson, R. E. & van Hamme, W. 2009, *ApJ*, 699, 118
- Wilson, R. E., van Hamme, W., & Terrell, D. 2010, *ApJ*, 723, 1469
- Wolf, M., & Zejda, M. 2005, *A&A*, 437, 545
- Worthey G., Lee H., 2011, *ApJS*, 193, 1
- Wyithe, J. S. B. & Wilson, R. E. 2002, *ApJ*, 571, 293

APPENDIX
TEMPERATURES AND REDDENING
V570 PER

The temperature of the system V570 Per was determined from a model atmosphere analysis of disentangled spectra (Tomasella et al. 2008b). Although formal errors on the temperatures quoted by the authors are very small (lower than 0.5%), the intrinsic colors of the components $b-y$, $B-V$, $V-J$ and $V-K$, point to much lower temperatures (by about 300 K), unless there is significantly larger interstellar extinction to this object than assumed by Tomasella et al. (2008b): $E(B-V) = 0.07$ mag instead of 0.023 ± 0.007 mag. There are two ways of resolving the problem: (1) the temperatures are indeed lower, or (2) the reddening is indeed higher. The first possibility would force us to assume that some error was made by Tomasella et al. (2008b) during their atmospheric analysis. This seems quite unlikely, however: (a) their atmospheric analysis is standard, (b) the spectra are of good quality, (c) higher temperatures correspond well with the components' spectral types and masses. Thus the more probable explanation of disagreement is possibility (2). However, it was reported that the interstellar potassium line KI (7699 Å) is not detected in the spectra of the system, which would contradict the higher reddening. Because we cannot solve this problem at the moment, for the purpose of this work, we kept the temperatures from Tomasella et al. (2008b) and assumed a reddening of 0.07 ± 0.03 mag to V570 Per. This problem clearly needs some future attention and more detailed investigation.

WW AUR

The temperatures of the components of WW Aur were previously determined by Smalley et al. (2002) and Southworth et al. (2005). However, $b-y$, $B-V$, $V-K$ colors suggest larger temperatures by about ~ 200 K, what was already pointed out by Southworth et al. (2005) in regard of the $b-y$ color. Wilson & van Hamme (2009) used their direct distance estimate (DDE) method and also found the temperatures of both components to be higher by a very similar amount. In our model we employed those higher temperatures.

KX CNC

For the system KX Cnc we determined the temperature from Strömgren uvby photometry ($b-y=0.378$; Olsen 1983) and Johnson's BVJK photometry. The temperature of the primary component derived from the different colors is as follows: $T_{b-y} = 5938$ K, $T_{B-V} = 5985$ K, $T_{V-J} = 6131$ K, $T_{V-K} = 6162$ K. The resulting mean temperature is $T_1 = 6050$ K i.e. larger by 150 K (1.5σ) than the original temperature T_1 derived by Sowell et al. (2012). The larger value is in better agreement with the original HD spectral classification: F8 (Cannon & Pickering 1919). Using the calibration between effective temperature and spectral type for normal main sequence stars (Pecaut & Mamajek 2013) we reclassify the system as F9V+F9V.

RZ CHA

The case of RZ Cha is interesting. Andersen et al. (1975) combined their velocimetry with Strömgren photometry obtained by Jørgensen & Gyldenkerne (1975) to derive "mean" parameters of the components. The reason behind it was their conclusion that the components of the system had very similar physical appearance and thus also parameters. This "indistinguishability" of components was retained by Torres et al. (2010) in their review. However, it is clear from inspection of the light curves that the components have different surface temperatures which was reported already by Giuricin et al. (1980). The difference is small, with the more massive and larger star being cooler by ~ 50 K, but it has an effect on the predicted infrared light ratios.

WZ OPH

The system was quite recently analyzed by Clausen et al. (2008a). They reported the temperature $T_1 = 6165 \pm 100$ K, based on reddening $E(B-V) = 0.044$ mag, intrinsic Strömgren color of the primary $(b-y)_0 = 0.329$ and a calibration by Holmberg et al. (2007). They noted that the temperature derived from atmospheric analysis of the disentangled primary's spectrum is slightly higher, however they did not report how much higher. From unreddened colors $b-y$, $B-V$, $V-K$ we derived also a higher temperature of $T_1 = 6301$ K (1.4σ difference). Lower reddening of $E(B-V) = 0.030$ mag resulting from Schlegel et al. (1998) maps leads to the temperature $T_1 = 6232$ K, a value which one would consider "slightly" higher. These values of reddening and temperatures are assumed in this work.

UZ DRA

Using B, V, J, K photometry we redetermined temperatures of both components because the original temperatures given by Lacy et al. (1989) were estimated only from the mean spectral type of the system. Resulting temperatures are higher by about 200 K than those reported by Lacy et al. (1989) and correspond much better with the masses of both components, which seem to be unevolved main-sequence stars.

VZ CEP

There is an inconsistency between the temperatures based on $B-V$, $b-y$ colors and $V-K$, $V-J$ with the NIR colors resulting in temperatures higher by about 300 K. Different values of reddening does not resolve the discrepant temperatures. A possible reason is that 2MASS magnitudes are somehow affected, however they were taken well outside of eclipses and all have an "A" flag. Higher temperatures would be in agreement with relatively massive components of the system, and furthermore the resulting photometric distance would be in perfect agreement with Hipparcos and Gaia parallaxes. However, we have no clue at this moment about the possible source of the discrepancy. We therefore retained in this paper the temperatures from the work by Torres & Lacy (2009), which are based on Strömgen photometry.

RADIAL VELOCITIES

V570 PER

Tomasella et al. (2008b) did not report radial velocity semiamplitudes. We utilized data from their Table 2 to rederive the orbital parameters. Our semi-major axis is larger by 1.5σ than value by Tomasella et al. (2008b) which we attribute mostly to a different choice of astrophysical constants, but our mass ratio q is fully consistent with their value.

HD 71636

Henry et al. (2006) reported two sets of radial velocity semiamplitudes in their Table 3 and Table 5 that contradict each other. Thus we rederived the spectroscopic orbit from the data in their Table 2. Our semiamplitudes are in perfect agreement with the values presented in Table 3 and we accordingly adopted them here.

KX CNC

Sowell et al. (2012) reported two sets of $K_{1,2}$ that contradict each other. Using the data from their Table 2 we determined the spectroscopic orbit that is fully consistent with the solution given in their Table 3.

V4089 SGR

Recently, Veramendi & González (2015) presented light and radial velocity curves solution of the system and they derived its absolute dimensions. However, the semi-major axis a reported in their Table 1 is inconsistent with their radial velocity semiamplitudes $K_{1,2}$ and masses. Our solution to the velocimetry kindly provided by M. Veramendi confirms their masses and $K_{1,2}$, but not their a . Also our K_2 is slightly larger (by 1.2σ); this is probably caused by the fact that we allowed for different systemic velocities for the components. Finally, we recalculated errors on the fundamental parameters which are significantly different from those reported in the Tables 1 and 2 by Veramendi & González (2015).

EF AQR

In paper by Vos et al. (2012) were presented fundamental physical parameters of the system. However, they reported two different sets of radial velocity semiamplitudes $K_{1,2}$ (their Tables 4 and 8). Using their velocimetry we redetermined spectroscopic orbits for this system. Our $K_{1,2}$ are much closer to the values presented in Table 8, but they are still somewhat different. Especially the epoch of spectroscopic conjunction is different in our solution by 0.002 days suggesting some period change in the system. We also recalculated fractional radii from the sum of radii and k given in their Table 6. The resulting radii and errors are again somewhat different from those reported in Table 6. Here we refer only to parameters that we have recalculated.

V821 CAS

Çakirli et al. (2009) reported their radial velocity measurements of the system. Their data in Table 1 are relatively noisy compared to preset-day standards, nevertheless, we rederived the spectroscopic orbits in order to verify the consistency of the orbital parameters and quoted errors. The radial velocity semiamplitudes from our solution are marginally consistent with their values and the overall agreement of the orbit is satisfactory, also regarding the assumed errors.